To determine whether synthetic siRNAs might induce DNA methylation in mammalian cells, we synthesized siRNAs targeted to CpG islands of the E-cadherin promoter (E-cadherin-siRNAs), as E-cadherin can be silenced by aberrant methylation of the promoter in several lines of tumour cells[17–19]. Moreover, as CpG sites in the E-cadherin promoter are unmethylated in MCF-7 cells[17,18], we chose MCF-7 cells for this study. We selected ten CpG sites (sites 1–10) in the E-cadherin promoter as targets of siRNAs (Fig. 1a). Each E-cadherin-siRNA (100 nM) was introduced into MCF-7 cells and, 96 h later, total DNA was collected and genomic DNA was isolated. We then performed bisulphite sequencing to determine the methylation status of the E-cadherin promoter. We treated genomic DNA with bisulphite using a CpGenome DNA-modification kit (Intergen). We amplified the bisulphite-modified E-cadherin promoter by polymerase chain reaction (PCR) and cloned the product of PCR using a TA cloning kit (Clontech). We picked ten independent colonies for each target site and analysed the cloned sequences by direct sequencing.

As shown in Fig. 1b, we found methylated DNA in MCF-7 cells that harboured each respective E-cadherin-siRNA (sites 1–10) and cells harbouring all E-cadherin-siRNAs (sites 1–10; the number of grey squares indicates the number of methylated cytosines). By contrast, a mutant form of the E-cadherin-siRNA directed against site 1 that had eight point mutations in both its sense and antisense strand failed to induce methylation. Moreover, a combination of all E-cadherin-siRNAs together failed to induce DNA methylation within a non-targeted *erbB2* promoter (Supplementary Fig. S1), highlighting the specificity of the E-cadherin-siRNAs. We next examined the possibility of methylation beyond the target site in the absence of RNA-directed RNA polymerase (RdRP) in mammalian cells. Notably, siRNAs targeted to site 3 of the E-cadherin promoter induced methylation not only at that site but also at the adjacent site (site 2), at least to some extent (Fig. 1c). However, site 1, located ~200 nucleotides upstream of site 3, was unmethylated.

Aberrant methylation is often detected in cancer cells. Therefore, we next examined the induction of DNA methylation by siRNAs in normal breast epithelial cells. We detected methylation of CpG sites in normal breast epithelial cells that had been treated with E-cadherin-siRNAs (testing methylation at sites 6 and 10; Supplementary Fig. S2). Furthermore, the extent of methylation in MCF-7 cells that had been treated with a combination of all ten E-cadherin-siRNAs was reduced in the presence of 1 μM 5-aza-2′-deoxycytidine (5-aza), an inhibitor of DNA methylation (Fig. 1d).

As methylation of histone H3 at lysine 9 is induced by RNAi in plants, fission yeast and *Drosphila*[8,20,21], we examined whether our set of siRNAs could induce its methylation in mammalian cells using a chromatin immunoprecipitation assay with specific antibodies for methylated histone H3 at lysine 9. Each cell lysate from MCF-7 cells and normal mammary epithelial cells in the presence or absence of the E-cadherin-siRNAs (sites 1–10) was incubated with specific antibodies for methylated histone H3 at lysine 9 or antibodies for histone H3, and the DNA interacting with the methylated histone H3 was immunoprecipitated. The precipitated DNA was then amplified using specific primers for the E-cadherin promoter. As shown in Fig. 1e, the precipitated DNA from the cell lysate of E-cadherin-siRNA-treated MCF-7 cells produced a band corresponding to the E-cadherin promoter region. By contrast, we did not detect the corresponding band when the same procedure was performed in the absence of E-cadherin-siRNAs or in the presence of mutant siRNAs. Similar results were obtained using cell lysate from normal mammary epithelial cells. In addition, it has been reported that an RNA component is involved in maintenance or stabilization of a higher-order structure at pericentric heterochromatin in mammalian cells[22].

Taken together, these results suggest that siRNAs targeted to the E-cadherin promoter can induce not only DNA methylation but also histone H3 methylation at lysine 9 in human cancer cells and normal cells, and that the effects of siRNAs can spread to nearby regions even in the absence of RdRP.

To examine whether the induction of DNA methylation by E-cadherin-siRNAs was correlated with expression of the E-cadherin gene, we performed northern blotting analysis with a probe specific

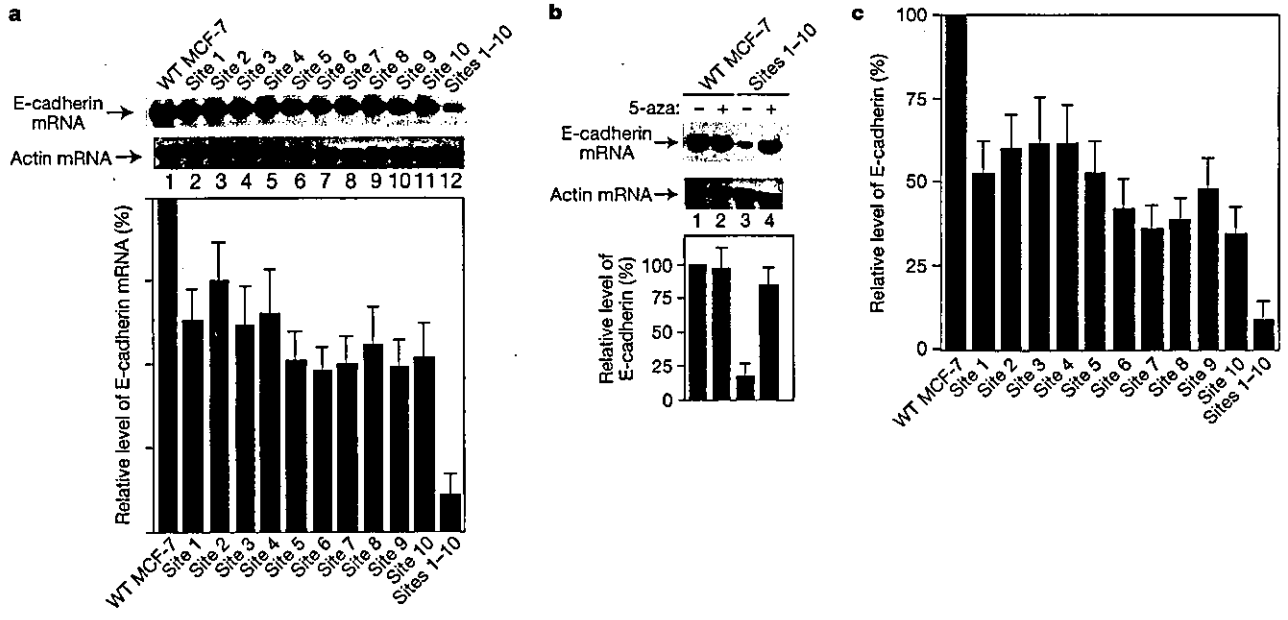

Figure 2 Effects of E-cadherin-siRNAs targeted to the E-cadherin promoter on E-cadherin mRNA expression. **a**, Levels of E-cadherin mRNA expression in cells transfected with E-cadherin-siRNAs. Total RNA from each line was analysed by northern blotting analysis. Actin mRNA was used as the endogenous control. Values are means ± s.d. **b**, Relative levels of E-cadherin mRNA expression in cells transfected with E-cadherin-siRNAs and grown with and without 5-aza. **c**, Levels of E-cadherin expression in cells transfected with E-cadherin-siRNAs. E-cadherin in each line was detected by western blotting with specific antibodies. Relative levels of E-cadherin were analysed densitometrically. Values are means ± s.d.

for E-cadherin mRNA. As shown in Fig. 2a, the level of E-cadherin mRNA expression in each line of MCF-7 cells harbouring a specific E-cadherin-siRNA was lower than in wild-type MCF-7 cells (lanes 1–11). Notably, the level of E-cadherin mRNA expression in MCF-7 cells that had been treated with a combination of all E-cadherin-siRNAs (lane 12) was significantly lower than in MCF-7 cells transfected with a single siRNA, clearly demonstrating the additive effects of the siRNAs. Treatment with 5-aza almost completely abolished the effect of the E-cadherin-siRNAs (Fig. 2b, lane 4). Western blot analysis with an E-cadherin-specific antibody also revealed similar reductions in the amount of E-cadherin (Fig. 2c). Thus, siRNAs targeted to the E-cadherin promoter act as gene silencers at the transcriptional level, and induction by siRNAs of DNA methylation within the E-cadherin promoter is inversely correlated with the level of gene expression and is additive.

DNA methyltransferases (DNMTs) are responsible for all DNA methylation in the cell[23–25]. To determine whether DNMTs participate in siRNA-mediated DNA methylation in human cells, we tried to suppress the expression of genes for DNMTs using siRNAs targeted to the respective mRNAs. We synthesized three separate siRNAs that targeted to *DNMT1*, *DNMT2* and *DNMT3B* mRNAs, respectively. As controls, we used mutant *DNMT1*-, *DNMT2*- and *DNMT3B*-siRNAs with four point mutations in both the sense and antisense strand. We introduced *DNMT*-siRNA or mutant *DNMT1*-siRNA at 100 nM into MCF-7 cells using Oligofectamine, and examined the amount of DNMTs by western blotting. Amounts of DNMT1, DNMT2 and DNMT3B in MCF-7 cells transfected with *DNMT1*-siRNA, *DNMT2*-siRNA or *DNMT3B*-siRNA, respectively, but not the corresponding mutant *DNMT*-siRNAs, were significantly lower than those in wild-type MCF-7 cells (Fig. 3a).

To examine whether reduced expression of DNMT genes affects siRNA-mediated DNA methylation, we introduced a combination of E-cadherin-siRNAs (sites 1–10) into MCF-7 cells transfected with *DNMT1*-, *DNMT2*- or *DNMT3B*-siRNAs. As shown in Fig. 3b, the extent of DNA methylation induced by E-cadherin-siRNAs in MCF-7 cells transfected with *DNMT1*- and *DNMT3B*-siRNA was significantly lower than in wild-type MCF-7 cells or in MCF-7 cells transfected with mutant *DNMT*-siRNA. By contrast, disruption of *DNMT2* expression did not significantly affect siRNA-mediated DNA methylation. Thus, *DNMT1* and *DNMT3B*, but not *DNMT2*, seem to be necessary for siRNA-mediated DNA methylation in human cells.

We next examined the effects of E-cadherin-siRNAs on the expression of E-cadherin in MCF-7 cells transfected with *DNMT*-siRNA. As shown in Fig. 3c, siRNAs targeted to the E-cadherin promoter did not alter E-cadherin gene expression in MCF-7 cells that contained siRNAs targeted to *DNMT1* or *DNMT3B* mRNA (lanes 4 and 16). By contrast, E-cadherin-siRNAs suppressed

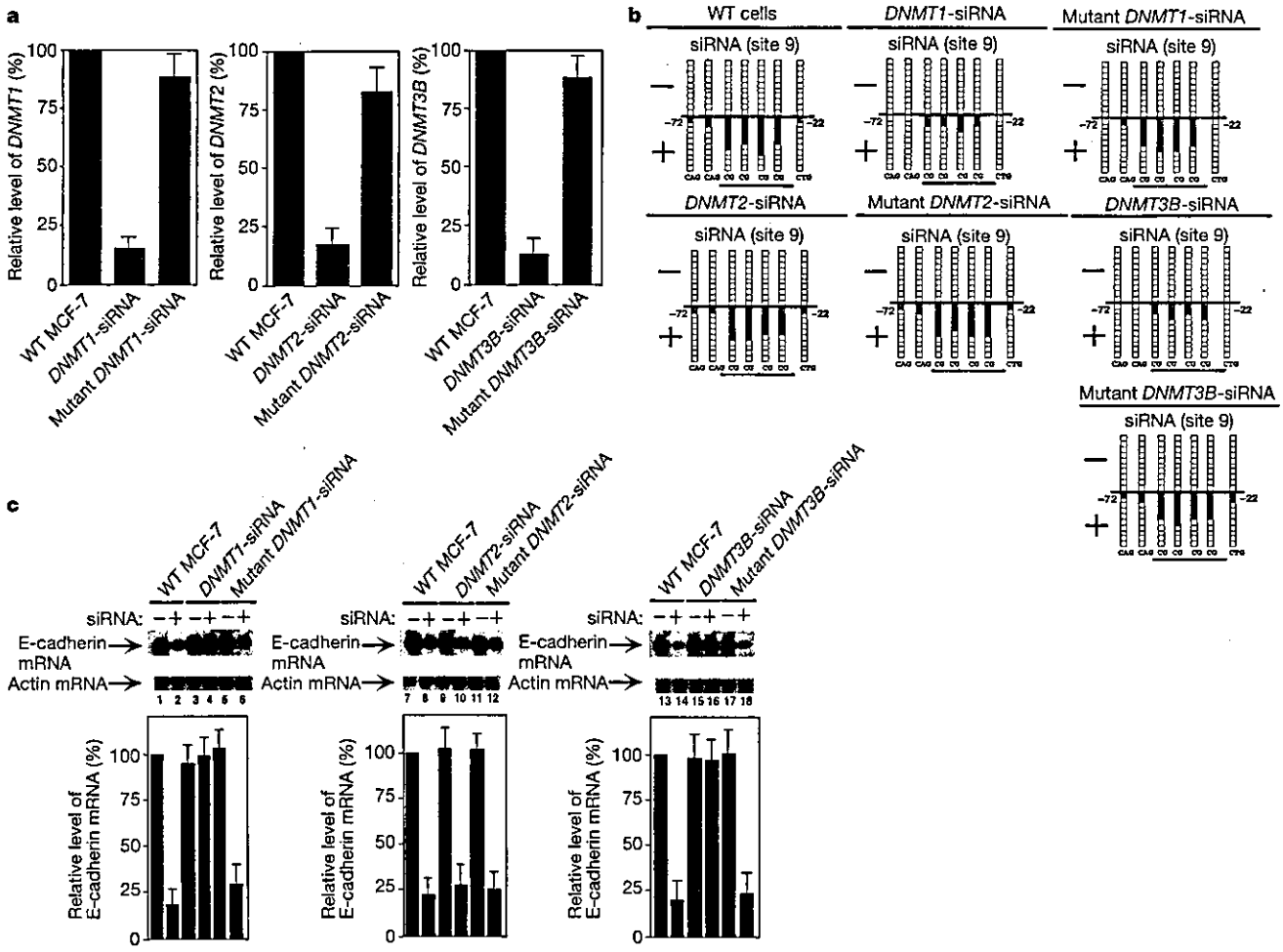

Figure 3 Effects of E-cadherin-siRNAs targeted to the E-cadherin promoter in DNMT1-, DNMT2- and DNMT3B-knockdown cells. **a**, Amount of DNMTs in MCF-7 cells in the presence or absence of *DNMT*-siRNAs. The amount of DNMT1, DNMT2 and DNMT3B was detected by western blotting. Values are means ± s.d. **b**, Level of DNA methylation of the E-cadherin promoter in MCF-7 cells in the presence or absence of E-cadherin-siRNA and various *DNMT*-siRNAs. DNA methylation was detected by bisulphite sequencing. **c**, E-cadherin mRNA expression levels in MCF-7 cells in the presence or absence of E-cadherin-siRNA (sites 1–10) and various *DNMT*-siRNAs. Total RNA from each line was analysed by northern blotting with specific probes. Values are means ± s.d.

E-cadherin gene expression in MCF-7 cells that contained *DNMT2*-siRNA or mutant *DNMT*-siRNAs (lanes 6, 10, 12 and 18), demonstrating that *DNMT1* and *DNMT3B* are necessary for the transcriptional gene silencing that results from the induction of DNA methylation by E-cadherin-siRNAs.

To examine the possibility for gene therapy via the control of DNA methylation by siRNAs, we constructed expression vectors for short hairpin RNAs (shRNAs) targeted to an *erbB2* promoter. The *erbB2* gene is overexpressed and unmethylated in several lines of tumour cells, such as MCF-7 cells, whereas it can be silenced by methylation of the promoter in several lines of normal cells[26]. To express shRNAs in cells, we used the well-characterized $tRNA^{Val}$ promoter system[16]. We have demonstrated previously that $tRNA^{Val}$-driven shRNA induces siRNA-mediated gene silencing in human cells[16]. We selected five CpG islands (sites 1–5) within the *erbB2* promoter as targets of shRNAs. Then, we introduced these shRNA expression plasmids transiently into MCF-7 cells. We confirmed by means of northern blotting that appropriate processing and production of siRNAs had occurred in cells that expressed tRNA-shRNAs (Fig. 4b, lanes 1–5), and then we examined levels of DNA methylation within the *erbB2* promoter. We isolated genomic DNA from each cell line and performed bisulphite sequencing. As shown in Fig. 4c, we detected DNA methylation within the *erbB2* promoter in all lines of MCF-7 cells that expressed a tRNA-shRNA or a combination of all tRNA-shRNAs (sites 1–5). However, a mutant tRNA-shRNA (site 1) with nine point mutations in both the sense and antisense strand did not induce DNA methylation within the *erbB2* promoter. In addition, tRNA-shRNA did not induce DNA methylation within the non-targeted E-cadherin promoter (Supplementary Fig. S3). We obtained similar results with U6 promoter-driven shRNAs (data not shown), demonstrating that induction of sequence-specific DNA methylation by vector-based siRNAs in human cells is a general phenomenon.

To determine whether the vector-based shRNAs had suppressed the expression of *erbB2*, we examined levels of *erbB2* mRNA expression by means of northern blotting. As shown in Fig. 4d, the expression level of *erbB2* mRNA in cells that expressed each respective tRNA-shRNA was lower than in wild-type MCF-7 cells.

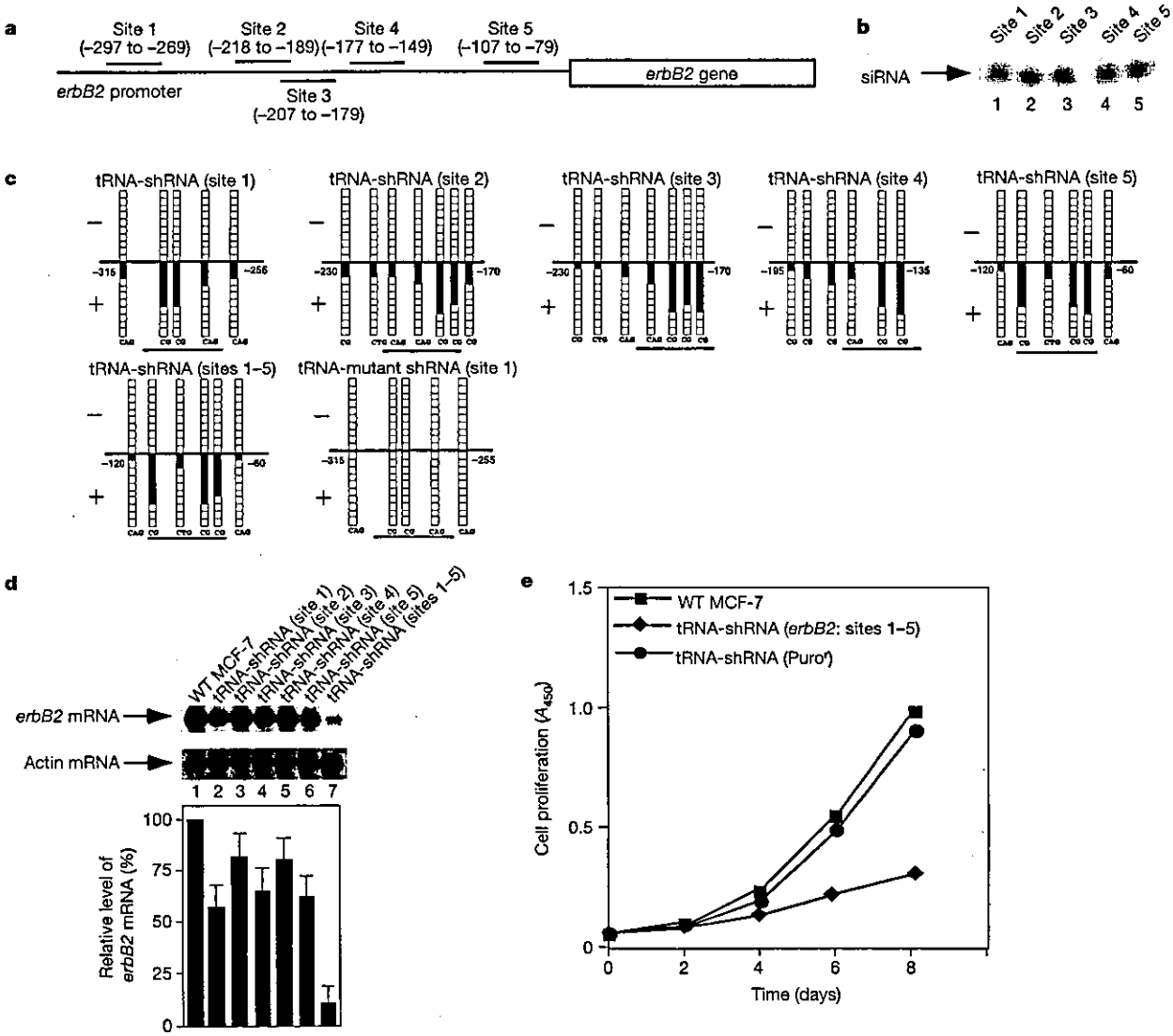

Figure 4 Induction of DNA methylation of the *erbB2* promoter by tRNA-shRNAs. **a**, Five targets for tRNA-shRNAs were selected within the *erbB2* promoter. **b**, Detection, via northern blots, of the expression of tRNA-shRNAs targeted to the *erbB2* promoter. All anticipated siRNAs were detected in cells that expressed tRNA-shRNAs. **c**, Induction by shRNAs of DNA methylation of the *erbB2* promoter, as detected by bisulphite sequencing. **d**, Relative levels of *erbB2* mRNA in cells that expressed tRNA-shRNAs targeted to the *erbB2* promoter. Total RNA from each line was analysed by northern blotting with specific probes. Values are means ± s.d. **e**, Proliferation rates of cells expressing tRNA-shRNAs. tRNA-shRNA (puro^r), targeted to a puromycin-resistance gene, was used as a control shRNA.

As observed previously (Fig. 2a), the level of *erbB2* mRNA expression in cells that expressed all tRNA-shRNAs (sites 1–5) together was significantly lower than in wild-type MCF-7 cells and in cells that expressed individual tRNA-shRNAs, demonstrating the additivity of suppression by vector-based shRNAs at the transcriptional level. Transcriptional regulation through the induction of methylation within a promoter by siRNA in mammalian cells seems to be a general phenomenon, as demonstrated by the examples in this study.

To examine the phenotype of cells that expressed tRNA-shRNAs, we analysed the proliferation rates of various cell lines. MCF-7 cells expressing all tRNA-shRNAs (sites 1–5) proliferated significantly more slowly than wild-type MCF-7 cells and cells that expressed tRNA-shRNAs targeted to a puromycin-resistance gene, which we chose as a nonspecific control (Fig. 4e). The reduced proliferation rate of MCF-7 cells that expressed all tRNA-shRNAs (sites 1–5) was correlated with a reduction in the level of *erbB2* mRNA expression in these cells, suggesting that the tRNA-shRNAs targeted to the *erbB2* promoter might have potential utility as therapeutic agents.

The DNA methylation of promoters has an important role in the genesis and development of tumours by regulating the expression of specific genes[27,28]. Many proteins involved in DNA methylation, such as MeCP2, MBD and DNMTs, have been well characterized in human cells. However, it remains unclear how and under what circumstances they are guided to and methylate specific CpG target sites of cognate genes during the genesis or development of tumours.

In plants, long and short dsRNAs can induce sequence-specific DNA methylation, known as RNA-directed DNA methylation[3–8]. In addition, transgenes can also induce sequence-specific DNA methylation[29,30]. These phenomena might reflect the role of these systems as a cellular defence against RNA and DNA viruses. However, it remains to be determined whether similar RNA-directed DNA methylation and transgene-mediated defence systems exist in human cells.

We have demonstrated that synthetic and vector-based siRNAs can induce sequence-specific and *DNMT1*/*DNMT3B*-dependent RNA-mediated DNA methylation in human cells. Our siRNAs induced sequence-specific gene silencing at the transcriptional level. The ways in which siRNAs are guided to and gain access to genomic DNA remain unknown. Synthetic and tRNA vector-based siRNAs are localized predominantly in the cytoplasm, where siRNA-mediated degradation of mRNA also occurs. A small fraction of siRNA–protein complexes might be transported to the nucleus. Alternatively, siRNAs might gain access to genomic DNA during cell division, when the nuclear membrane disappears.

Further investigation of correlations between siRNA-induced DNA methylation and tumour genesis, anti-viral defence and epigenesis in development should provide an insight into small-RNA-induced gene silencing and development. Moreover, it is now possible to control the expression levels of specific genes in mammalian cells using siRNAs not only to disrupt cognate mRNAs but also to interfere with transcription, as demonstrated here. However, it remains to be examined precisely which promoters can be specifically methylated by respective siRNAs. Exploitation of shRNA expression vectors targeted to cognate promoters might even have potential utility in a clinical setting. □

Methods

Preparation of siRNAs

Synthetic siRNAs directed against the E-cadherin promoter (E-cadherin-siRNA) and against DMNT mRNAs (DMNT-siRNAs) were synthesized with a DNA/RNA synthesizer (model 394; PE Applied Biosystems). Sequences of E-cadherin-siRNAs are described in the Supplementary Information. For generation of siRNAs, all synthetic RNAs were annealed by the standard method[15]. We introduced siRNAs into MCF-7 cells using Oligofectamine (Invitrogen) in accordance with the manufacturer's protocol.

Construction of tRNA-shRNA expression plasmids

To construct vectors for expression of tRNA-shRNA targeted to the *erbB2* promoter, we used the pPUR-tRNA plasmid, which includes a chemically synthesized promoter for a human gene for $tRNA^{Val}$ between the *Eco*RI and *Bam*HI sites of pPUR (Clontech)[16]. Sequences (sites 1–5) of shRNAs targeted to the *erbB2* promoter are described in Supplementary Information. Chemically synthesized oligonucleotides encoding *erbB2* promoter-directed shRNAs that included a loop motif were amplified as double-stranded sequences by PCR. After digestion with *Sac*I and *Kpn*I, the fragments were cloned downstream of the promoter of the $tRNA^{Val}$ gene in pPUR-tRNA.

Bisulphite sequencing of E-cadherin and *erbB2* promoters

We extracted genomic DNA from cells by standard methods using proteinase K, phenol and chloroform. We performed bisulphite modifications using a CpGenome DNA modification kit (Intergen) following the manufacturer's instructions. We amplified the bisulphite-modified E-cadherin and *erbB2* promoters using specific primers as follows: for the E-cadherin promoter, forward primer 5′-TCTAGAAAAATTTTTTAAAAA-3′ and reverse primer 5′-CAGCGCCGAGAGGCTGCGGCT-3′; for the *erb*B2 promoter, forward primer 5′-CCTGGAAGCCACAAGGTAAAC-3′ and reverse primer 5′-TTTCTCCGGTCCCAATGGAGG-3′. The amplified DNAs were subcloned into the TA-cloning vector. Then we picked ten independent colonies in each case, determined the sequence of the promoter in each plasmid and examined the extent of methylation by determining the number and position of methylated cytosine residues.

Culture and transfection of cells

Human MCF-7 cells were cultured in minimum essential medium (MEM) supplemented with 10% FCS, 1% NEAA and 1 mM Na-Pyr. Human normal mammary epithelial cells (CAMBREX) were grown with mammary epithelial cell medium (CAMBREX). Transfection with pPUR-tRNA-shRNA was performed with the Effectene reagent (Qiagen) according to the manufacturer's protocol. For transfection of MCF-7 cells with various siRNAs, we used Oligfectamine (Invitrogen) according to the manufacturer's protocol.

5-aza-2′-deoxycytidine treatment

For inhibition of DNA methylation by 5-aza-2′-deoxycytidine (5-aza), cells grown to 30–40% confluence were transfected with E-cadherin-siRNAs and then were incubated for 96 h in culture medium that contained a final concentration of 1 μM 5-aza (Sigma).

Northern blotting analysis

Total RNA was purified from MCF-7 cells that expressed tRNA-shRNAs targeted to the *erbB2* promoter with ISOGEN reagent (Wako). Thirty micrograms of total RNA per lane were loaded on a 15% polyacrylamide gel. After electrophoresis, bands of RNA were transferred to a Hybond-N nylon membrane (Amersham). The RNA on the membrane was allowed to hybridize to ^{32}P-labelled probes that were complementary to the sequences of the tRNA-shRNAs. Sequences of synthetic probes were as follows: site 1, 5′-CUCUG CCCCCUCCCCCGGAGUCCGGGAUAA-3′; site 2, 5′-UCCUAGCGCCGGGAAGCU GGGUUGCCUGCA-3′; site 3, 5′-GGUGCGUCCCUCCUAGCGCCGGGAAGCUGG-3′; site 4, 5′-GGUGCGUCCCUCCUAGCGCCGGGAAGCUGG-3′; and site 5, 5′-GAGCAA GCGCGCUCCCAGCUCGCCCCCUCC-3′. For detection of the expression level of E-cadherin, *erbB2* and actin mRNAs, we used cDNA probes of E-cadherin, *erbB2* and actin, respectively.

Western blotting analysis

MCF-7 cells transfected with or without various E-cadherin-siRNAs targeted to the E-cadherin promoter and various tRNA-shRNAs targeted to the *erbB2* promoter were collected. Total protein (20 μg) was fractionated by SDS–polyacrylamide gel electrophoresis (10% polyacrylamide) and bands of protein were transferred to a polyvinylidene difluoride membrane (Funakoshi) by electro-blotting. Immunocomplexes were visualized with an ECL kit (Amersham) after reactions with monoclonal antibodies against E-cadherin (Transduction laboratories), ErbB2 (Oncogene), actin (Chemicon), DNMT1 (Imgenex) and DNMT3B (Imgenex), or with polyclonal antibodies against DNMT2 (Imgenex). Amounts of E-cadherin and ErbB2 were normalized by reference amounts of actin.

Determination of cell proliferation rates

Cell proliferation rates were determined with a Cell Proliferation Kit II (Roche) according to the manufacturer's instructions[16].

Received 18 March; accepted 26 July 2004; doi:10.1038/nature02889.
Published online 15 August 2004.

1. Fire, A. *et al.* Potent and specific genetic interference by double-stranded RNA in *Caenorhabditis elegans*. *Nature* 391, 806–811 (1998).
2. Hutvagner, G. & Zamore, P. D. RNAi: nature abhors a double-strand. *Curr. Opin. Genet. Dev.* 12, 225–232 (2002).
3. Pelissier, T. & Wassenegger, M. A DNA target of 30 bp is sufficient for RNA-directed DNA methylation. *RNA* 6, 55–65 (2000).
4. Mette, M. F., Aufsatz, W., van der Winden, J., Matzke, M. A. & Matzke, A. J. Transcriptional silencing and promoter methylation triggered by double-stranded RNA. *EMBO J.* 19, 5194–5201 (2000).
5. Jones, L., Ratcliff, F. & Baulcombe, D. C. RNA-directed transcriptional gene silencing in plants can be inherited independently of the RNA trigger and requires Met1 for maintenance. *Curr. Biol.* 11, 747–757 (2001).

6. Hamilton, A., Voinnet, O., Chappell, L. & Baulcombe, D. Two classes of short interfering RNA in RNA silencing. *EMBO J.* **21**, 4671–4769 (2002).
7. Aufsatz, W., Mette, M. F., Van Der Winden, J., Matzke, M. & Matzke, A. J. HDA6, a putative histone deacetylase needed to enhance DNA methylation induced by double-stranded RNA. *EMBO J.* **21**, 6832–6841 (2002).
8. Zilberman, D., Cao, X. & Jacobsen, S. E. *ARGONAUTE4* control of locus-specific siRNA accumulation and DNA and histone methylation. *Science* **299**, 716–719 (2003).
9. Bernstein, E., Caudy, A. A., Hammond, S. M. & Hannon, G. J. Role for a bidentate ribonuclease in the initiation step of RNA interference. *Nature* **409**, 363–366 (2001).
10. Elbashir, S. M., Lendeckel, W. & Tuschl, T. RNA interference is mediated by 21- and 22-nucleotide RNAs. *Genes Dev.* **15**, 188–200 (2001).
11. Zamore, P., Tuschl, T., Sharp, P. & Bartel, D. RNAi: double-stranded RNA directs the ATP-dependent cleavage of mRNA at 21- to 23-nucleotide intervals. *Cell* **101**, 25–33 (2000).
12. Hammond, S. M., Bernstein, E., Beach, D. & Hannon, G. J. An RNA-directed nuclease mediates post-transcriptional gene silencing in *Drosophila* cells. *Nature* **404**, 293–296 (2000).
13. Elbashir, S. M. *et al.* Duplexes of 21-nucleotide RNAs mediate RNA interference in mammalian cell culture. *Nature* **411**, 494–498 (2001).
14. Hutvagner, G. & Zamore, P. D. A microRNA in a multiple-turnover RNAi enzyme complex. *Science* **297**, 2056–2060 (2002).
15. Zeng, Y. & Cullen, B. R. RNA interference in human cells is restricted to the cytoplasm. *RNA* **8**, 855–860 (2002).
16. Kawasaki, H. & Taira, K. Short hairpin type of dsRNAs that are controlled by $tRNA^{Val}$ promoter significantly induce RNAi-mediated gene silencing in the cytoplasm of human cells. *Nucleic Acids Res.* **31**, 700–707 (2003).
17. Herman, J. G., Graff, J. R., Myohanen, S., Nelkin, B. D. & Baylin, S. B. Methylation-specific PCR: a novel PCR assay for methylation status of CpG islands. *Proc. Natl Acad. Sci. USA* **93**, 9821–9826 (1996).
18. Graff, J. R., Herman, J. G., Myohanen, S., Baylin, S. B. & Vertino, P. M. Mapping patterns of CpG island methylation in normal and neoplastic cells implicates both upstream and downstream regions in *de novo* methylation. *J. Biol. Chem.* **272**, 22322–22329 (1997).
19. Corn, P. G. *et al.* E-cadherin expression is silenced by 5′ CpG island methylation in acute leukemia. *Clin. Cancer Res.* **6**, 4243–4248 (2000).
20. Volpe, T. A. *et al.* Regulation of heterochromatic silencing and histone H3 lysine-9 methylation by RNAi. *Science* **297**, 1833–1837 (2002).
21. Pal-Bhadra, M. *et al.* Heterochromatic silencing and HP1 localization in *Drosophila* are dependent on the RNAi machinery. *Science* **303**, 669–672 (2004).
22. Maison, C. *et al.* Higher-order structure in pericentric heterochromatin involves a distinct pattern of histone modification and an RNA component. *Nature Genet.* **30**, 329–334 (2002).
23. Bestor, T. H. The DNA methyltransferases of mammals. *Hum. Mol. Genet.* **9**, 2395–2402 (2000).
24. Rhee, I. *et al.* DNMT1 and DNMT3b cooperate to silence genes in human cancer cells. *Nature* **416**, 552–556 (2002).
25. Robert, M. F. *et al.* DNMT1 is required to maintain CpG methylation and aberrant gene silencing in human cancer cells. *Nature Genet.* **33**, 61–65 (2003).
26. Hattori, M., Sakamoto, H., Satoh, K. & Yamamoto, T. DNA demethylase is expressed in ovarian cancers and the expression correlates with demethylation of CpG sites in the promoter region of c-erbB-2 and survivin genes. *Cancer Lett.* **169**, 155–164 (2001).
27. Li, E. Chromatin modification and epigenetic reprogramming in mammalian development. *Nature Rev. Genet.* **3**, 662–673 (2002).
28. Esteller, M. CpG island hypermethylation and tumor suppressor genes: a booming present, a brighter future. *Oncogene* **21**, 5427–5440 (2002).
29. Morel, J. B., Mourrain, P., Beclin, C. & Vaucheret, H. DNA methylation and chromatin structure affect transcriptional and post-transcriptional transgene silencing in *Arabidopsis*. *Curr. Biol.* **10**, 1591–1594 (2000).
30. Beclin, C., Boutet, S., Waterhouse, P. & Vaucheret, H. A branched pathway for transgene-induced RNA silencing in plants. *Curr. Biol.* **12**, 684–688 (2002).

Supplementary Information accompanies the paper on **www.nature.com/nature.**

Acknowledgements This research was supported by grants from AIST and by a Grant-in-Aid for Scientific Research and for the 21st Century COE programmes, Center for Integrated Brain Medical Science and Human-Friendly Materials based on Chemistry, from the Ministry of Education, Culture, Sports, Science and Culture (MEXT) of Japan.

Competing Interests statement The authors declare that they have no competing financial interests.

Correspondence and requests for materials should be addressed to K.T. (taira@chembio.t.u-tokyo.ac.jp) or H.K. (kawasaki@chembio.t.u-tokyo.ac.jp).

Differentiation (2004) 72:58–64

REVIEW

Hiroaki Kawasaki · Renu Wadhwa · Kazunari Taira

World of small RNAs: from ribozymes to siRNA and miRNA

Received November 7, 2003; accepted December 11, 2003

Abstract RNAs, besides bridging genetic information to proteins, the major determinants of bio-structures and functions, serve as active regulators of gene expression. Initiated nearly 20 years ago with ribozymes (the small RNAs with catalytic activity providing fine tuning of gene expression and function, used as molecular scissors and tools for gene discovery), an era of more complex and coordinated gene regulation by small RNAs, siRNA, and miRNA has recently started. Simple nucleotide complementarity results in highly ordered and regulated events, such as assembly of RNA and proteins, resulting in gene silencing either by mRNA degradation or suppression of translation. This article reviews our contributions to the understanding of structure, the function of small RNAs, their use in biotechnology, and the understanding of phenotypes such as apoptosis, metastasis, and differentiation.

Key words ribozymes · siRNA · miRNA · regulation of gene expression · neuronal differentiation

The world of small RNA inaugurated by the ribozyme: from gene silencing to gene discovery

RNA was previously viewed as a mere bridge between DNA (reservoir of all genetic information) and protein (determinants of biological structure, function, and integrity). Its perception as a simple vehicle for deciphering the genetic code to a translatable readout changed about 20 years ago when RNA with catalytic activity, ribozyme—RNA molecule with enzymatic properties—were discovered. Hammerhead ribozymes (because of the resemblance of their two-dimensional structure to a hammerhead) are the smallest ribozymes that are used as molecular scissors in molecular biology and biotechnology to elucidate and eliminate gene functions (Haseloff and Gerlach, 1988; Rossi, 1999). The RNA is induced to fold into its active conformation by the binding of metal ions. It forms two domains: the scaffold (domain 2), on which the ribozyme is built, and the active center (catalytic domain called domain 1) of the ribozyme. Over the last two decades, mechanisms of action of hammerhead ribozymes describing the requirement of divalent metal ions, definition of catalytic domains, and sequence specificity (usually referred to as target site specificity) have been largely demonstrated (Minoshima et al., 2003).

Ribozyme activity *in vivo* critically depends on its effective level of expression, specificity, intracellular stability, target co-localization, and accessibility to the target site. These technical issues impose a major difficulty in the use of ribozymes *in vivo*. Various modifications of plasmids to express ribozymes in cells have thus come into play. It was shown that the ribozymes expressed under the control of a modified RNA polymerase III promoter ($tRNA^{Val}$ promoter) were efficiently expressed, highly stable, and exported to the cytoplasm (Koseki et al., 1999; Kato et al., 2001; Kuwabara et al., 2001a, 2001b). Such expression improved ribozyme activity *in vivo* by many fold. However, efficiently expressed and highly stable ribozymes may still lack activity due to their inaccessibility to the target sites that in turn impose a major hurdle because of unforeseeable secondary and tertiary RNA structures. The rate-limiting step for the cleavage of phosphodiester bonds *in vivo* is the association and annealing of the ribozyme with its target site (Kato et al., 2001; Warashina et al., 2001; Kawasaki et al.,

Hiroaki Kawasaki · Kazunari Taira(✉)
Department of Chemistry and Biotechnology
School of Engineering
The University of Tokyo
7-3-1 Hongo, Bunkyo-ku
Tokyo 113-8656, Japan
Tel: +81-3-5841-8828
Fax: +81-3-5841-8828
E-mail: taira@chembio.t.u-tokyo.ac.jp

Hiroaki Kawasaki · Renu Wadhwa · Kazunari Taira
Gene Function Research Center
National Institute of Advanced Industrial Science and Technology (AIST)
Central 4, 1-1-1 Higashi
Tsukuba Science City 305-8562, Japan

2002). In a long RNA molecule, with its secondary and tertiary folded structure, a significant number of target sites are inaccessible to the ribozyme. This phenomenon is often a serious problem in attempts to exploit ribozyme activity, in particular *in vivo*. To overcome the problems of accessibility, computer-generated predictions of secondary structure can be typically used to identify target sites that are most likely to be in an open and accessible conformation. However, such predictions are not always accurate because of unpredictable interactions between RNAs and proteins that influence the intracellular structures of RNAs.

A significant recent modification of ribozymes that overcomes their target inaccessibility has been demonstrated. In this modification, a helicase-binding motif that recruits helicase protein and its unwinding activity *in vivo* was linked to the 3′ end of the ribozyme sequence in the RNA polymerase III promoter ($tRNA^{Val}$)-driven expression plasmid (Warashina et al., 2001; Kawasaki and Taira, 2002a; Fig. 1). Such RNA helicase-coupled ribozymes were indeed shown to have substrate-unwinding as well as strong cleavage activity in *in vitro* and *in vivo* assays (Warashina et al., 2001; Kawasaki and Taira, 2002a; Kawasaki et al., 2002) and were effective where conventional ribozymes did not cause any change in gene expression (Wadhwa et al., 2003). Subsequent to this significant modification of ribozymes, it became possible to prepare effective libraries of hybrid ribozymes with randomized binding arms and to examine their effects after being introduced into cells (Kawasaki and Taira, 2002b; Kawasaki et al., 2002; Suyama et al., 2003a, 2003b). This led us to develop a novel approach for cloning functional genes. Briefly, libraries of hybrid ribozymes in which the target arm sequence was randomized were generated. These were introduced into cells by either plasmid or retroviral vectors and were combined with the selection of a loss or gain of a cellular phenotype. Isolation of ribozymes from selected cells, sequence analysis, and identification of genes in databases could lead to the identification of genes involved in these phenotypes (Fig. 2). The application of the ribozyme-based gene discovery system to apoptosis, metastasis, Alzheimer's disease, and muscle differentiation led to the isolation of several genes that are implicated in these phenotypes, confirming the validity and usefulness of this technology (Kruger et al., 2000; Li et al., 2000; Welch et al., 2000; Beger et al., 2001; Kawasaki and Taira, 2002a, 2002b; Kawasaki et al., 2002; Nelson et al., 2003; Suyama et al., 2003a, 2003b; Onuki et al., 2004; R.W. et al., unpublished data). Besides, many novel genes have been isolated, supporting it as an effective tool to isolate new genes and elucidate novel functional pathways. This system has also led to the isolation of small RNAs involved in regulation of neuronal differentiation (T. Kuwabara et al., personal communication).

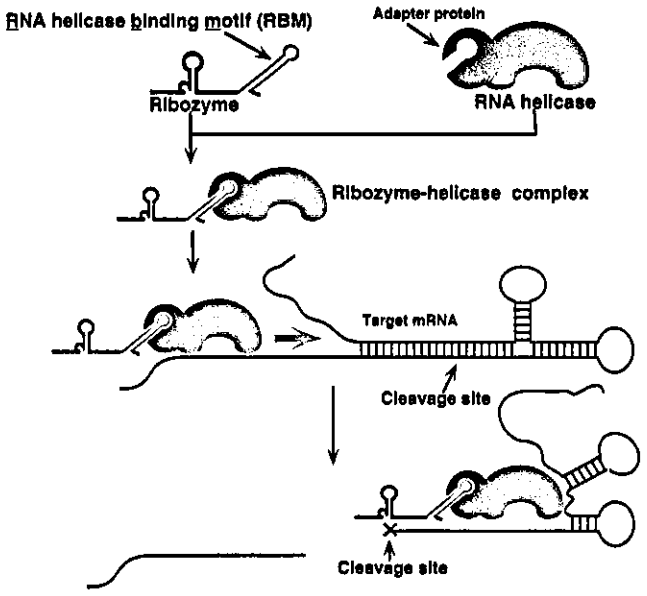

Fig. 1 Schematic representation of cleavage of a normally inaccessible target site by a sliding hybrid ribozyme. The ribozyme is linked to an RNA helicase-binding motif (RBM or connector RNA) that is capable of recruiting a helicase(s) to the target site where it unwinds the substrate structure to expose the cleavage site. The helicase might even be able to slide the ribozyme along the transcript. The coupling of helicase activity to the ribozyme allows suppression of the expression of genes whose transcripts were found previously resistant to cleavage by the conventional ribozyme.

Another significant modification of ribozymes was the construction of allosterically controllable ribozymes that bind to two different target sites (Kuwabara et al., 1999). Such ribozymes were effectively used for suppression of genetic disorders that arise from gene

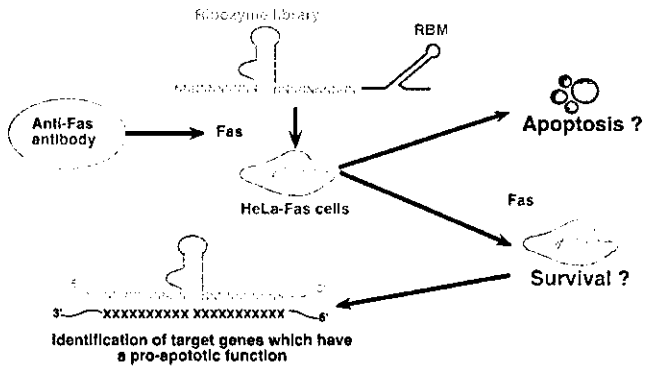

Fig. 2 Schematic presentation of a gene discovery system that can identify functional genes in the Fas-mediated pathway to apoptosis. Randomized RBM-connected ribozyme libraries were introduced into HeLa-Fas cells using the retrovirus expression system. After infection with the randomized RBM-Rz library expressing retrovirus, HeLa-Fas cells that expressed the randomized library were treated with Fas-specific antibody (α-Fas). Surviving clones were picked up and genomic DNA was purified from each clone. Sequences of RBM-connected ribozyme were determined by direct sequencing and the target genes of ribozymes were identified in databases by a BLAST search.

rearrangements. For example, chronic myelogenous leukemia is a hematopoietic malignant disease associated with the expression of a chimeric *BCR-ABL* gene. A ribozyme that can disrupt chimeric *BCR-ABL* mRNA exclusively and is neutral to normal *ABL* mRNA was designed and shown to specifically cleave *BCR-ABL* mRNA (Kuwabara et al., 1998; Tanabe et al., 2000).

The world of small RNA extended to siRNA and miRNA

In the post-genome era, when curiosity in the field of biology centered on "how gene expression and function are regulated," an amazing discovery in biological regulation flashed in science news and made its way to the top scientific journals. The articles, "brave new world of RNA," "a small fortune," "tiny regulators with great potential," "small RNAs: the genome's guiding hand," "something new under the sun," "breakthrough of the year," "small RNAs make big splash," and "big things from little RNA" talked about regulation of gene expression by small RNAs (Ambros, 2001; Couzin, 2002; Moss and Poethig, 2002; Pasquinelli, 2002; Moberg and Hariharan, 2003). These tiny regulators come from the large proportion of non-coding genome referred to as junk DNA and regulate the fate of cells, not by coding for any proteins with functional motifs, but by causing gene silencing by a highly coordinated and sequence-specific mechanism known as RNA interference (RNAi) and/or micro-RNA-mediated regulation. Small RNAs, including microRNAs (miRNAs) and short interfering RNAs (siRNAs), have emerged as the key components of an evolutionarily conserved system of RNA-based gene regulation in eukaryotes. They are involved in molecular interactions, including defense against viruses and regulation of gene expression during development (Cullen, 2002; Carrington and Ambros, 2003). How these 21- to 23-nucleotide (nt) small non-coding RNAs can act as small interfering RNAs (siRNAs) or miRNAs is just beginning to be understood. The two kinds of small RNAs, that is, siRNAs and miRNAs, are produced by the cleavage of double-stranded RNA precursors by Dicer, a member of the RNase III family of dsRNA-specific endonucleases (Bernstein et al., 2001; Provost et al., 2002; Zhang et al., 2002). siRNAs are 21-nt double-stranded RNAs that contain 19 base pairs, with 2-nt, 3′ overhanging ends, that act as functional intermediates in RNAi. These are formed in cells when transposons, viruses, or endogenous genes express long dsRNA or when dsRNA is introduced experimentally. In contrast, single-stranded miRNAs are the products of endogenous, non-coding genes whose precursor RNA transcripts can form small stem loops from which mature miRNAs are produced by Dicer (Ambros et al., 2003; Lim et al., 2003a, 2003b). miRNAs are encoded in genes distinct from the mRNAs whose expression they control. In contrast to siRNA, which can direct RNA destruction mediated by RISC (RNA-induced silencing complex; functions as an siRNA-directed endonuclease), miRNAs suppress protein expression by inhibition of mRNA translation (Fig. 3). Because both siRNAs and miRNAs are found in similar, if not identical, complexes, it is suggested that RISC might be a bi-functional complex that mediates both cleavage and translational control (Mourelatos et al., 2002). Furthermore, recent evidence suggests that siRNAs and miRNAs are functionally interchangeable, in which the target mRNA can be either cleaved or translationally repressed as determined by the degree of complementarity between the small RNA and its target (Hutvágner and Zamore, 2002; Doench et al., 2003; Zeng et al., 2003).

MicroRNAs (*miR* genes) are a large family of highly conserved non-coding genes transcribed as short hairpin precursors (~70 nt) that are processed into active 21- to 22-nt RNAs by a ribonuclease, Dicer, which recognizes target mRNAs via base-pairing interactions. The miRNA-miRNP (ribonucleoprotein) complex represses mRNA translation by partial base pairing to the 3′ UTR of target mRNAs. Small RNA of 18–25 bases called microRNA (miRNA) was reported for the first time by the group of Victor Ambros (Dartmouth College) in 1993. They found that miRNA that interacts with the 3′ UTR of *lin-4* mRNA regulates nematode

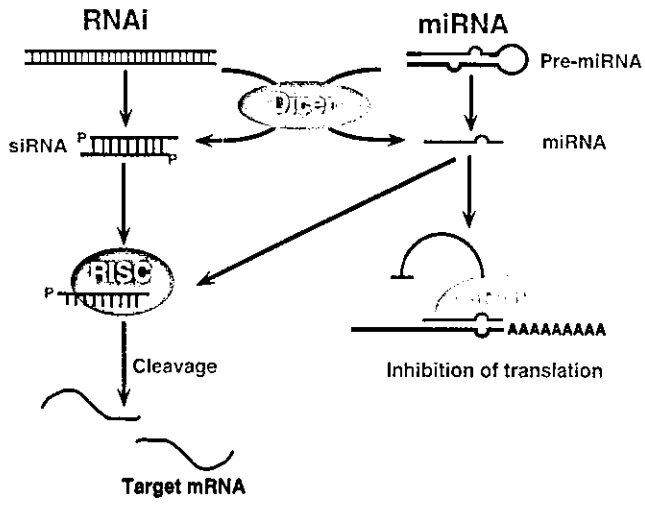

Fig. 3 Diagram to show siRNA and miRNA action. siRNAs are produced from long dsRNAs by ribonuclease Dicer. Then siRNAs are incorporated in RISC and the RISC cleaves the target RNAs. MicroRNAs are expressed as short hairpin RNAs (pre-miRNAs) and are transported to the cytoplasm. Pre-miRNAs are processed to mature miRNAs by Dicer. The miRNAs are incorporated in miRNPs and then miRNPs inhibit translation of target mRNAs by forming partial duplexes with target mRNAs. In addition, miRNA can function as siRNAs in the case of complete matching with target mRNAs.

development. Similarly, miRNA to *let-7* mRNA was identified. Both *lin-4* and *let-7* act as repressors of their respective target genes, such as *lin-14*, *lin-28*, and *lin-41*. Both *lin-4* and *let-7* small temporal RNAs were shown to play a central role in controlling the timing of *Caenorhabditis elegans* cell fate decisions. *let-7* has been conserved through evolution, and its expression correlates with adult development in animals, including *Drosophila* (Bashirullah et al., 2003). A best match for *lin-4* in *Drosophila*, miR-125, is also expressed during pupal and adult stages of *Drosophila* development (Sempere et al., 2003). To date, over 300 miRNAs from diverse eukaryotic organisms have been identified. Annotation of new miRNAs, so that miRNAs can be reliably distinguished from siRNAs, has been proposed along with the establishment of the Rfam database of RNA families (Ambros, 2001, 2003; Ambros et al., 2003; Grad et al., 2003). How these tiny RNAs work is only beginning to be understood; the major hurdle is to identify their target mRNAs. The fact that makes it even more arduous is that miRNA require only a partial homology (in some cases, about 70%). Some of the *Drosophila* miRNAs that align to the K box motif were shown to mediate a negative post-transcriptional regulation of the Hairy *HES* gene family in *Drosophila* (Lai and Posakony, 1997; Lai et al., 1998; Lai, 2002). The human miR-23 containing the antisense sequence to the K box motif was also identified, of which the target gene is not known.

We initiated a study to investigate whether human Hairy *HES* gene is the target of human miR-23 (Kawasaki and Taira, 2003). HES1 is a basic helix-loop-helix (bHLH) transcriptional repressor that is expressed in undifferentiated cells but not in differentiated cells (Kageyama et al., 2000). It participates in the Notch signaling pathway in mammals and acts as an anti-differentiation factor. miR-23 aligns to a coding region of human *HES1* mRNA near the termination codon and to mouse *Hes1* mRNA (nearly the same position as human *HES1* including the stop codon; Fig. 4a). A duplex of *HES1* and miR-23 was also observed using a prediction program of mRNA secondary structure (Mulfold), suggesting that miR-23 may be conserved phylogenetically as a regulator of human and mouse Hes1.

We used NT2 cells as a model for neuronal differentiation. When subjected to retinoic acid (RA)-induced differentiation, NT2 cells showed suppression of Hes1 expression that was independent of the level of mRNA, as detected by Northern analysis. miR-23, on the other hand, was easily detected in differentiated NT2 cells in contrast to undifferentiated cells. Introduction of the synthetic wild-type miR-23, but not the mutant miR-23, into undifferentiated NT2 cells resulted in the reduction of Hes1 protein. Of note, the level of *HES1* mRNA did not change in response to the synthetic miR-23, suggesting that synthetic miR-23

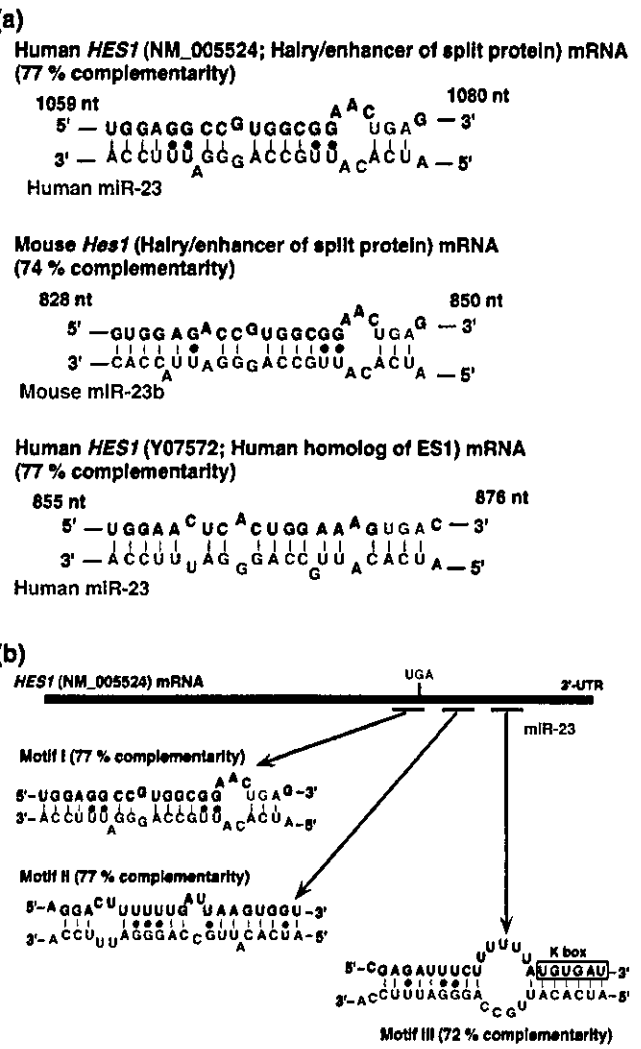

Fig. 4 HES1 is a target of miR-23. (a) The prediction of secondary structures between miR-23 and its target RNAs. The region nearly complementary to human and mouse miR-23 (blue) is located in the coding region, near the termination codon (red) of human Hairy *HES1* (NM_005524), mouse *Hes1*, and human homolog *HES1* (Y07572) mRNAs (top). (b) Human Hairy *HES1* (NM_005524) mRNA has three target regions (motifs I, II, and III) of miR-23 (bottom). Motif III has a K box sequence (black box) that is known, at least in the case of *Drosophila*, to be involved in post-transcriptional negative regulation.

causes gene silencing at the translational level. As expected, targeting of endogenous miR-23 by synthetic siRNA (siRNA-miR-23) indeed resulted in an elevation of HES1 protein, but the mutant siRNA-miR-23 had no effect. These data strongly support that HES1 is a target for miR-23. NT2 cells did not undergo RA-induced neuronal differentiation (as confirmed by cell morphology and differentiation markers such as MAP2) in the presence of siRNA-miR-23, suggesting that miR-23 plays a critical role during RA-induced neuronal differentiation of NT2 cells. The functional regulation of *HES1* by an miRNA mechanism was further confirmed by using two more miRNA motifs (Fig. 4b)

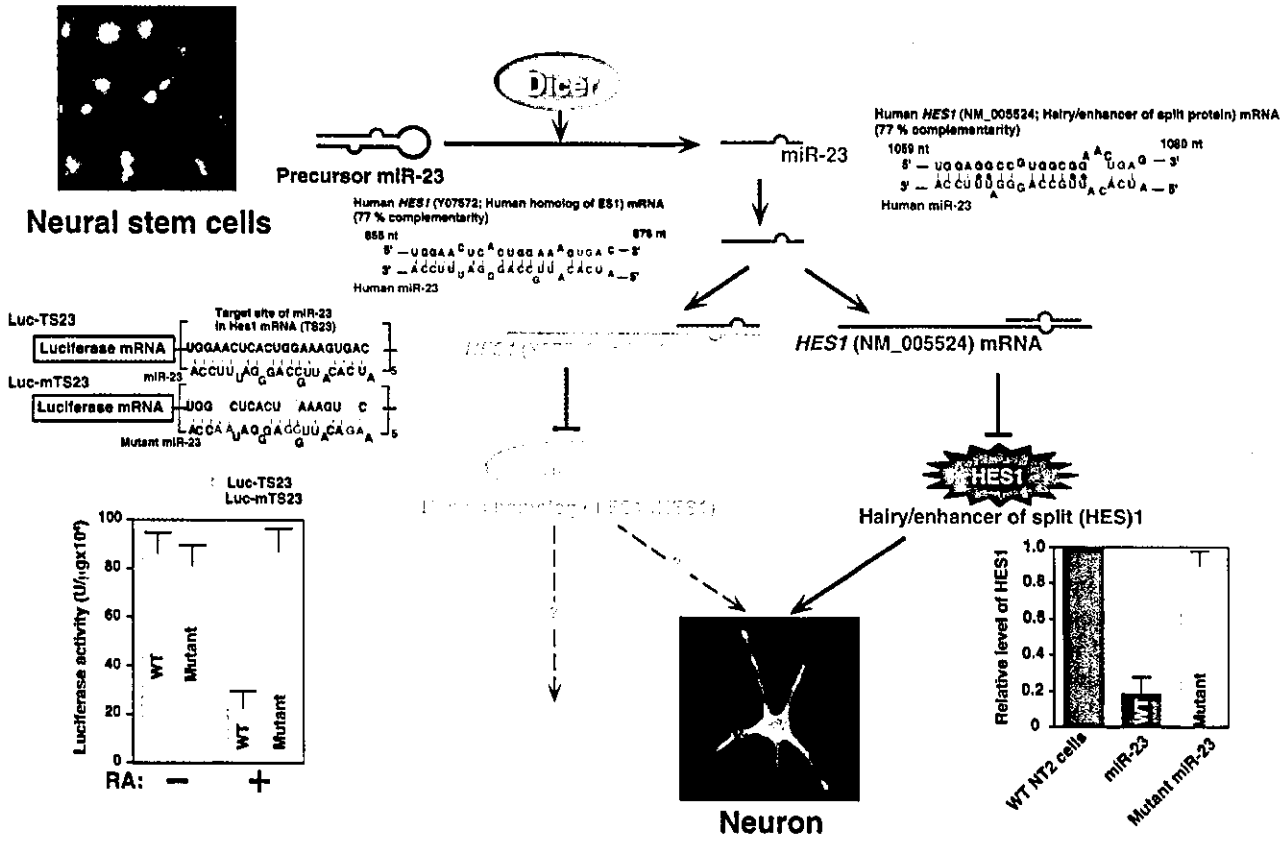

Fig. 5 The model of the function of miR-23 in RA-induced differentiation. When cells were treated with RA, pre-miR-23 is expressed. Then the pre-miR-23 is processed to mature miR-23 by ribonuclease Dicer. The mature miR-23 negatively regulates expression of Hairy *HES1* gene strongly and homolog *HES1* gene weakly. Then these events promote neuronal differentiation of NT2 cells. Left lower panel: sequences of genes for Luc-TS23 and mutant Luc-TS23 (Luc-mTS23). The activity of luciferase, due to the reporter genes, in NT2 cells in the presence and absence of RA. Right lower panel: the level of Hes1 mRNA in undifferentiated NT2 cells that had been treated with synthetic miR-23 or synthetic mutant miR-23.

and their various combinations along with the original miR-23 (Figs. 4b,5), which happened to match another cDNA also called *HES1* (human homolog of *Escherichia coli* and zebrafish; GenBank accession number Y07572; Scott et al., 1997; Kawasaki and Taira, 2003; unpublished data). We were informed of this ambiguity by Debbie Marks (Columbia University). Hairy/enhancer of split protein, also called *HES1* gene (accession number NM_005524; Feder et al., 1994), which actually encodes the transcriptional repressor HES1, was the subject of our study and is referred to as Hairy *HES1* (Kawasaki and Taira, 2003). Of note, in our study, the HES1 protein was detected by anti-HES1 antibody and the miR-23 was seen to suppress HES1 protein levels (Kawasaki and Taira, 2003). Thus, although the database sequence homologies raise doubts on the validity of the data demonstrating hairy HES1 as a target for miR-23, protein analysis stands by it.

To further clarify this issue, we investigated the effect of two additional independent miRNA target motifs (Fig. 4b) that were found in the 3′ UTR of Hairy *HES1* mRNA and did not match to homolog *HES1* (Fig. 5). Analysis of the activity of the luciferase reporter that was linked to the 5′ end of the miR-23 target site or the sequence of the other two unique potential target motifs in Hairy *HES1* mRNA revealed that the three independent target motifs (Fig. 4b) act as targets of miR-23 in Hairy *HES1* mRNA; each of these sites have only about 72–77% homology to the target. Thus, although detoured by the long route of confirmation and validation, the consequence of the study remains unchanged in describing that HES1 is regulated by miRNA such as miR-23.

A model for the function of miR-23 in regulation of RA-induced neuronal differentiation of NT2 cells is proposed (Fig. 5). When cells were treated with RA, pre-miR-23 is expressed. The pre-miR-23 is then processed to mature miR-23 by the ribonuclease Dicer. The mature miR-23 negatively regulates expression of Hairy *HES1* gene strongly and homolog *HES1* gene weakly. These events then promote neuronal differentiation of NT2 cells. However, the mechanism of expression of pre-miR-23 and inhibition of translation of both *HES1* mRNAs by miR-23 remains to be addressed in future studies.

In an independent study, we were compelled to recall what we referred to as pseudo-positives in our screens to

search for novel genes using a ribozyme-based discovery system. Many of the target sequences were ignored and forgotten because they did not belong to the coding genome. Those of us who could not ignore the pseudo-positives won this time. T. Kuwabara et al. (2004) used a randomized ribozyme library to isolate genes involved in neuronal development and isolated small RNAs that determine the fate of cells. It is becoming clear that nature has structured sequence information to embed in it not only structural and functional aspects of proteins but also non-coding regulatory elements such as siRNA and miRNA. An era of an unexplored functional RNA world has begun, and is predicted to go a long way in providing information for the understanding of the regulation of biological phenotypes.

Note added in proof: Kawasaki, H. and Taira, K. (2003) Hes1 is a target of microRNA-23 during retinoic-acid-induced neuronal differentiation of NT2 cells. Nature 423, 838-842. In this Article, the mRNA that is identified to be a target of microRNA-23 (miR-23) is from the gene termed human 'homolog of ES1' (HES1), accessionnumber Y07572, and not from the gene encoding the transcriptional repressor Hairy enhancer of split HES1 (accession number NM_00524) as stated in this paper. We incorrectly identified the gene because of the confusing nomenclature. Our experiments in NT2 cells had revealed that the protein levels of the repressor Hes1 were diminished by miR-23. Although we have unpublished data that suggest that miR-23 also interacts with Hes1 repressor mRNA specially in NT2 cells, given the incorrect use of the probe for the detection of the target mRNA resulting from our error, we respectfully retracted this paper [Kawasaki, H. and Taira, K. (2003). retraction: Hes1 is a target of microRNA-23 during retinoic-acid-induced neuronal differentiation of NT2 cells. Nature *426*, 100].

Acknowledgments This study was partly supported by grants from the National Institute of Advanced Industrial Science and Technology (AIST), Japan.

References

Ambros, V. (2001) microRNAs: tiny regulators with great potential. Cell 107:823–826.

Ambros, V. (2003) MicroRNA pathways in flies and worms: growth, death, fat, stress, and timing. Cell 113:673–676.

Ambros, V., Bartel, B., Bartel, D.P., Burge, C.B., Carrington, J.C., Chen, X., Dreyfuss, G., Eddy, S.R., Griffiths-Jones, S., Marshall, M., Matzke, M., Ruvkun, G. and Tuschl, T. (2003) A uniform system for microRNA annotation. RNA 9:277–279.

Bashirullah, A., Pasquinelli, A.E., Kiger, A.A., Perrimon, N., Ruvkun, G. and Thummel, C.S. (2003) Coordinate regulation of small temporal RNAs at the onset of *Drosophila* metamorphosis. Dev Biol 259:1–8.

Beger, C., Pierce, L.N., Kruger, M., Marcusson, E.G., Robbins, J.M., Welcsh, P., Welch, P.J., Welte, K., King, M.C., Barber, J.R. and Wong-Staal, F. (2001) Identification of Id4 as a regulator of BRCA1 expression by using a ribozyme-library-based inverse genomics approach. Proc Natl Acad Sci USA 98: 130–135.

Bernstein, E., Caudy, A.A., Hammond, S.M. and Hannon, G.J. (2001) Role for a bidentate ribonuclease in the initiation step of RNA interference. Nature 409:363–366.

Carrington, J.C. and Ambros, V. (2003) Role of microRNAs in plant and animal development. Science 301:336–338.

Couzin, J. (2002) Breakthrough of the year. Small RNAs make big splash. Science 298:2296–2297.

Cullen, B.R. (2002) RNA interference: antiviral defense and genetic tool. Nat Immunol 3:597–599.

Doench, J.G., Petersen, C.P. and Sharp, P.A. (2003) siRNAs can function as miRNAs. Genes Dev 17:438–442.

Feder, J.N., Li, L., Jan, L.Y. and Jan, Y.N. (1994) Genomic cloning and chromosomal localization of HRY, the human homolog to the *Drosophila* segmentation gene, hairy. Genomics 20:56–61.

Grad, Y., Aach, J., Hayes, G.D., Reinhart, B.J., Church, G.M., Ruvkun, G. and Kim, J. (2003) Computational and experimental identification of *C. elegans* microRNAs. Mol Cell 11:1253–1263.

Haseloff, J. and Gerlach, W.L. (1988) Simple RNA enzymes with new and highly specific endonuclease activities. Nature 334: 585–591.

Hutvágner, G. and Zamore, P.D. (2002) A microRNA in a multiple-turnover RNAi enzyme complex. Science 297:2056–2060.

Kageyama, R., Ohtsuka, T. and Tomita, K. (2000) The bHLH gene Hes1 regulates differentiation of multiple cell types. Mol Cell 29:1–7.

Kato, Y., Kuwabara, T., Warashina, M., Toda, H. and Taira, K. (2001) Relationships between the activities *in vitro* and *in vivo* of various kinds of ribozyme and their intracellular localization in mammalian cells. J Biol Chem 276:15378–15385.

Kawasaki, H. and Taira, K. (2002a) Identification of genes by hybrid ribozymes that couple cleavage activity with the unwinding activity of an endogenous RNA helicase. EMBO Rep 3:443–450.

Kawasaki, H. and Taira, K. (2002b) A functional gene discovery in the Fas-mediated pathway to apoptosis by analysis of transiently expressed randomized hybrid-ribozyme libraries. Nucleic Acids Res 30:3609–3614.

Kawasaki, H. and Taira, K. (2003) Hes1 is a target of microRNA-23 during retinoic-acid-induced neuronal differentiation of NT2 cells. Nature 423:838–842.

Kawasaki, H., Onuki, R., Suyama, E. and Taira, K. (2002) Identification of genes that function in the TNF-α-mediated apoptotic pathway using randomized hybrid ribozyme libraries. Nat Biotechnol 20:376–380.

Koseki, S., Tanabe, T., Tani, K., Asano, S., Shioda, T., Nagai, Y., Shimada, T., Ohkawa, J. and Taira, K. (1999) Factors governing the activity *in vivo* of ribozymes transcribed by RNA polymerase III. J Virol 73:1868–1877.

Kruger, M., Beger, C., Li, Q.X., Welch, P.J., Tritz, R., Leavitt, M., Barber, J.R. and Wong-Staal, F. (2000) Identification of eIF2Bγ and eIFγ as cofactors of hepatitis C virus internal ribosome entry site-mediated translation using a functional genomics approach. Proc Natl Acad Sci USA 97:8566–8571.

Kuwabara, T., Warashina, M., Tanabe, T., Tani, K., Asano, S. and Taira, K. (1998) A novel allosterically trans-activated ribozyme, the maxizyme, with exceptional specificity *in vitro* and *in vivo*. Mol Cell 2:617–627.

Kuwabara, T., Warashina, M., Nakayama, A., Ohkawa, J. and Taira, K. (1999) $tRNA^{Val}$-heterodimeric maxizymes with high potential as gene inactivating agents: simultaneous cleavage at two sites in HIV-1 Tat mRNA in cultured cells. Proc Natl Acad Sci USA 96:1886–1891.

Kuwabara, T., Warashina, M., Sano, M., Tang, H., Wong-Staal, F., Munekata, E. and Taira, K. (2001a) Recognition of engineered tRNAs with an extended 3′ end by exportin-t (Xpo-t) and transport of tRNA-attached ribozymes to the cytoplasm in somatic cells. Biomacromol 2:1229–1242.

Kuwabara, T., Warashina, M., Koseki, S., Sano, M., Ohkawa, J., Nakayama, K. and Taira, K. (2001b) Significantly higher activity of a cytoplasmic hammerhead ribozyme than a corresponding nuclear counterpart: engineered tRNAs with an extended 3′ end can be exported efficiently and specifically to the cytoplasm in mammalian cells. Nucleic Acids Res 29:2780–2788.

Kuwabara, T., Hsieh, J., Nakashima, K., Taira, K. and Gag, F.H. (2004) A small modulatory dsRNA specifies the fate of adult neural stem cells. Cell (in Press).

Lai, E.C. (2002) Micro RNAs are complementary to 3′ UTR sequence motifs that mediate negative post-transcriptional regulation. Nat Genet 30:363–364.

Lai, E.C. and Posakony, J.W. (1997) The Bearded box, a novel 3′ UTR sequence motif, mediates negative post-transcriptional regulation of bearded and enhancer of split complex gene expression. Development 124:4847–4856.

Lai, E.C., Burks, C. and Posakony, J.W. (1998) The K box, a conserved 3′ UTR sequence motif, negatively regulates accumulation of enhancer of split complex transcripts. Development 125:4077–4088.

Li, Q.-X., Robbins, J.M., Welch, P.J., Wong-Staal, F. and Barber, J.R. (2000) A novel functional genomics approach identifies mTERT as a suppressor of fibroblast transformation. Nucleic Acids Res 28:2605–2612.

Lim, L.P., Glasner, M.E., Yekta, S., Burge, C.B. and Bartel, D.P. (2003a) Vertebrate microRNA genes. Science 299:1540.

Lim, L.P., Lau, N.C., Weinstein, E.G., Abdelhakim, A., Yekta, S., Rhoades, M.W., Burge, C.B. and Bartel, D.P. (2003b) The microRNAs of *Caenorhabditis elegans*. Genes Dev 17:991–1008.

Minoshima, H., Suyama, E., Wadhawa, R. and Taira, K. (2003) Use of hammerhead ribozymes for aging and cancer. In: Kaul, S.C. and Wadhawa, R. (eds.) Aging of Cells In and Outside the Body. Kluwer Academic Publishers, The Netherlands, pp. 257–267.

Moberg, K.H. and Hariharan, I.K. (2003) Big things from a little RNA. Trends Cell Biol 13:455–457.

Moss, E.G. and Poethig, R.S. (2002) MicroRNAs: something new under the sun. Curr Biol 12:R688–R690.

Mourelatos, Z., Dostie, J., Paushkin, S., Sharma, A., Charroux, B., Abel, L., Rappsilber, J., Mann, M. and Dreyfuss, G. (2002) miRNPs: a novel class of ribonucleoproteins containing numerous microRNAs. Genes Dev 16:720–728.

Nelson, L.D., Suyama, E., Kawasaki, H. and Taira, K. (2003) Use of random ribozyme libraries for the rapid screening of apoptosis or metastasis-related genes. Targets 2:191–200.

Onuki, R., Bando, Y., Suyama, E., Katayama, T., Kawasaki, H., Baba, T., Tohyama, M. and Taira, K. (2004) Involvement of an RNA-dependent protein kinase (PKR) in tunicamycin-induced apoptosis and Alzheimer's disease. EMBO J 23:959–968.

Pasquinelli, A.E. (2002) MicroRNAs: deviants no longer. Trends Genet 18:171–173.

Provost, P., Dishart, D., Doucet, J., Frendewey, D., Samuelsson, B. and Radmark, O. (2002) Ribonuclease activity and RNA binding of recombinant human dicer. EMBO J 21:5864–5874.

Rossi, J.J. (1999) Ribozymes, genomics and therapeutics. Chem Biol 6:R33–R37.

Scott, H.S., Chen, H., Rossier, C., Lalioti, M.D. and Antonarakis, S.E. (1997) Isolation of a human gene (HES1) with homology to an *Escherichia coli* and a zebrafish protein that maps to chromosome 21q22.3. Hum Genet 99:616–623.

Sempere, L.F., Sokol, N.S., Dubrovsky, E.B., Berger, E.M. and Ambros, V. (2003) Temporal regulation of microRNA expression in *Drosophila melanogaster* mediated by hormonal signals and broad-complex gene activity. Dev Biol 259:9–18.

Smallridge, R. (2001) A small fortune. Nat Rev Mol Cell Biol 2:867.

Suyama, E., Kawasaki, H., Nakajima, M. and Taira, K. (2003a) Identification of genes involved in cell invasion using a library of randomized hybrid ribozymes. Proc Natl Acad Sci USA 100:5616–5621.

Suyama, E., Kawasaki, H., Kasaoka, T. and Taira, K. (2003b) Identification of genes responsible for cell migration by a library of randomized ribozymes. Cancer Res 63:119–124.

Tanabe, T., Kuwabara, T., Warashina, M., Tani, K., Taira, K. and Asano, S. (2000) Oncogene inactivation in a mouse model. Nature 406:473–474.

Wadhwa, R., Ando, H., Kawasaki, H., Taira, K. and Kaul, S.C. (2003) Targeting mortalin using conventional and RNA-helicase-coupled hammerhead ribozymes. EMBO Rep 4:595–601.

Warashina, M., Kuwabara, T., Kato, Y., Sano, M. and Taira, K. (2001) RNA-protein hybrid ribozymes that efficiently cleave any mRNA independently of the structure of the target RNA. Proc Natl Acad Sci USA 98:5572–5577.

Welch, P.J., Marcusson, E.G., Li, Q.X., Beger, C., Kruger, M., Zhou, C., Leavitt, M., Wong-Staal, F. and Barber, J.R. (2000) Identification and validation of a gene involved in anchorage-independent cell growth control using a library of randomized hairpin ribozymes. Genomics 66:274–283.

Zeng, Y., Yi, R. and Cullen, B.R. (2003) MicroRNAs and small interfering RNAs can inhibit mRNA expression by similar mechanisms. Proc Natl Acad Sci USA 100:9779–9784.

Zhang, H., Kolb, F.A., Brondani, V., Billy, E. and Filipowicz, W. (2002) Human Dicer preferentially cleaves dsRNAs at their termini without a requirement for ATP. EMBO J 21:5875–5885.

Published online 9 August 2004

Nucleic Acids Research, 2004, Vol. 32, No. 14 4217–4223
doi:10.1093/nar/gkh753

Importance in catalysis of a magnesium ion with very low affinity for a hammerhead ribozyme

Atsushi Inoue[1,3], Yasuomi Takagi[1,2] and Kazunari Taira[1,2,3,*]

[1]Gene Function Research Center and [2]iGENE Therapeutics, Inc., National Institute of Advanced Industrial Science and Technology (AIST), Central 4, 1-1-1 Higashi, Tsukuba Science City 305-8562, Japan and [3]Department of Chemistry and Biotechnology, School of Engineering, The University of Tokyo, Hongo, Tokyo 113-8656, Japan

Received December 16, 2003; Revised and Accepted July 21, 2004

ABSTRACT

Available evidence suggests that Mg^{2+} ions are involved in reactions catalyzed by hammerhead ribozymes. However, the activity in the presence of exclusively monovalent ions led us to question whether divalent metal ions really function as catalysts when they are present. We investigated ribozyme activity in the presence of high levels of Mg^{2+} ions and the effects of Li^+ ions in promoting ribozyme activity. We found that catalytic activity increased linearly with increasing concentrations of Mg^{2+} ions and did not reach a plateau value even at 1 M Mg^{2+} ions. Furthermore, this dependence on Mg^{2+} ions was observed in the presence of a high concentration of Li^+ ions. These results indicate that the Mg^{2+} ion is a very effective cofactor but that the affinity of the ribozyme for a specific Mg^{2+} ion is very low. Moreover, cleavage by the ribozyme in the presence of both Li^+ and Mg^{2+} ions was more effective than expected, suggesting the existence of a new reaction pathway—a cooperative pathway—in the presence of these multiple ions, and the possibility that a Mg^{2+} ion with weak affinity for the ribozyme is likely to function in structural support and/or act as a catalyst.

INTRODUCTION

Naturally existing catalytic RNAs include hammerhead, hairpin, hepatitis delta virus (HDV) and Varkud Satellite (VS) ribozymes, group I and II introns, and the RNA subunit of RNase P (1–7). In addition, recent structural and chemical analyses strongly suggest that ribosomal RNA might also be a ribozyme (8–11). In addition, the possibility exists that the RNA component of the spliceosome might be a ribozyme too (12). The earliest research on ribozymes suggested that all ribozymes might be metalloenzymes that require divalent metal ions, in particular Mg^{2+} ions, for catalysis, and that all might operate by a basically similar mechanism. However, subsequent, extensive studies revealed that the catalytic activity of hairpin ribozymes is independent of divalent metal ions (7,13–18). Thus, the various types of ribozymes appear to exploit different cleavage mechanisms, which depend upon the architecture of the individual ribozyme. Even hammerhead ribozymes, which have generally been characterized as typical metalloenzymes, can no longer be categorized unambiguously.

Naturally existing hammerhead ribozymes were originally identified in some RNA viruses, and it was demonstrated that they act *in cis* during viral replication by the rolling circle mechanism (3). In the laboratory, ribozymes have been engineered such that they act *in trans* against other RNA molecules and catalyze the cleavage of phosphodiester bonds at specific sites to generate specific products, each of which has a 2′,3′-cyclic phosphate and a 5′-hydroxyl group (19–22). The transesterification mechanism includes deprotonation of the 2′-hydroxyl moiety of a ribose group, nucleophilic attack of the 2′-oxygen on the adjacent phosphorus atom, and protonation of the 5′-oxyanion leaving group (Figure 1A). A large body of evidence also indicates that the P9/$G_{10.1}$ site binds a metal ion with high affinity, with other metal ion-binding sites being located around the G_5 nucleobase and A_{13} phosphate near the site of cleavage (23–36). Thus, the idea that ribozymes are metalloenzymes has been generally accepted. However, it was reported recently that hammerhead ribozymes are active in the presence of very high concentrations of monovalent cations, such as Li^+ or NH_4^+ ions, in the absence of divalent metal ions (37). This finding raises the possibility that hammerhead ribozymes should not be classified as metalloenzymes. Therefore, we decided to investigate ribozyme activity in the presence of Mg^{2+} ions and the effects of Mg^{2+} ions in the presence of Li^+ ions on ribozyme activity, using a well-studied model hammerhead ribozyme (R32) and its substrate (S11), both of which are shown in Figure 1B (5–7,25,28,32–34,38–41).

We investigated the dependence on the concentration of Mg^{2+} and Li^+ ions of ribozyme activity over a range from 5 mM to ~1 M Mg^{2+} ions and 1 to 5 M Li^+ ions, respectively. Although several research groups have reported similar analyses (42–50), the concentrations of Mg^{2+} ions used in most of these studies were <100 mM, and little information is available about activity at a higher concentration, such as 1 M. The activity at high concentrations of Mg^{2+} ions, as compared

*To whom correspondence should be addressed at Department of Chemistry and Biotechnology, School of Engineering, The University of Tokyo, Hongo, Tokyo 113-8656, Japan. Tel: +81 3 5841 8828 or +81 29 861 3015; Fax: +81 29 861 3019; Email: taira@chembio.t.u-tokyo.ac.jp

The authors wish it to be known that, in their opinion, the first two authors should be regarded as joint First Authors

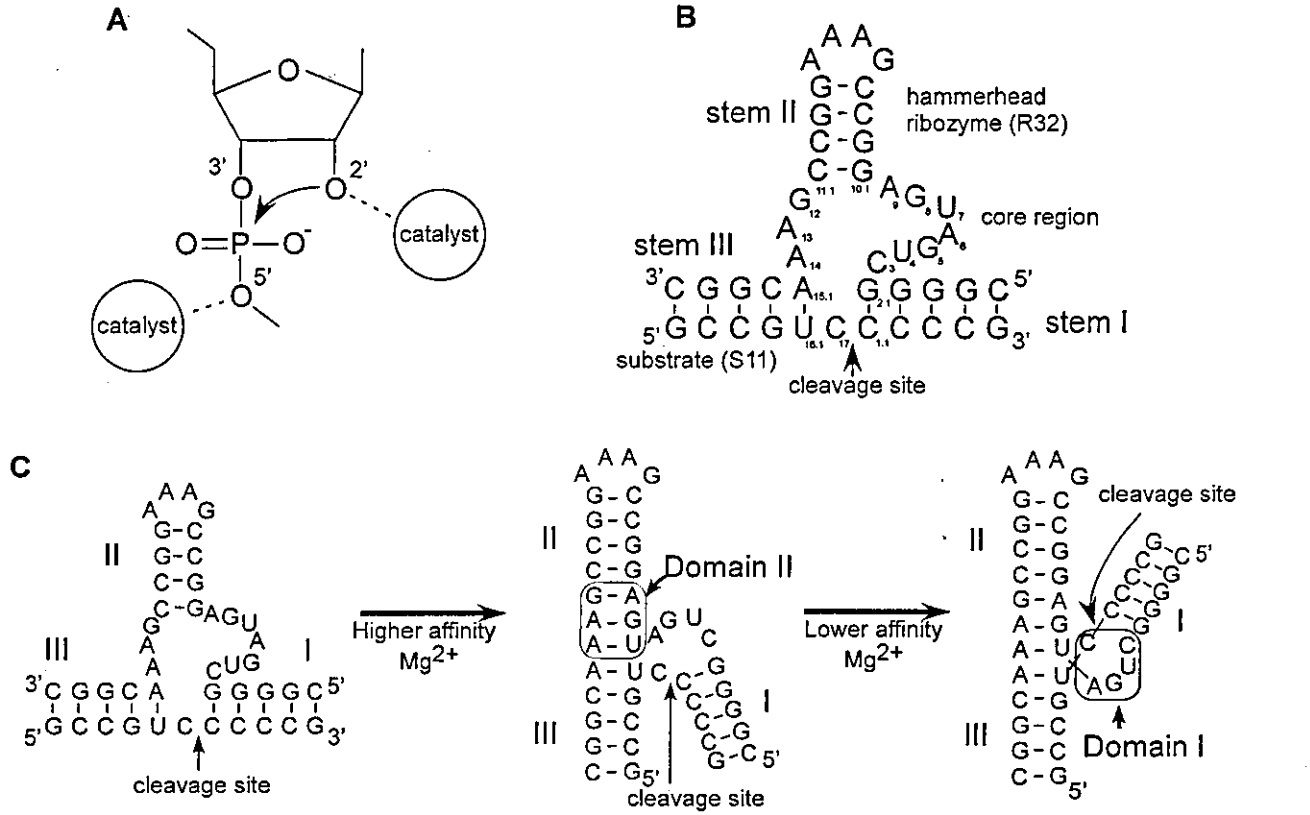

Figure 1. (A) Schematic representation of the proposed mechanism of the hammerhead ribozyme reaction. The 2′-hydroxyl moiety is activated by the catalyst and attacks the adjacent phosphate nucleophilically, with subsequent cleavage of the bond at the 5′-oxygen. The developing negative charge on the leaving 5′-oxygen is stabilized by another catalyst. (B) The sequences and secondary structures of the hammerhead ribozyme (R32) and substrate (S11) used in this study. (C) The proposed two-stage folding scheme for the hammerhead ribozyme–substrate complex. The higher-affinity Mg^{2+} ion(s) drives the formation of domain II, which contains non-Watson–Crick pairings and the lower-affinity Mg^{2+} ion(s) rotates around helix I, forming the catalytic core.

to physiological concentrations, is useful for studies of the chemistry of the hammerhead ribozyme and it allowed us to estimate the intrinsic cleavage rate constant and to compare an enzymatic reaction to a non-enzymatic reaction. We were also able to calculate acceleration energy more precisely and to investigate the dependence on Mg^{2+} ions in the presence of high concentrations of Li^{+} ions. Considering the results of such analyses, we propose the existence of a new cooperative pathway that involves divalent metal ions, such as Mg^{2+}, and monovalent ions, such as Li^{+}, in the reaction catalyzed by a hammerhead ribozyme. We also discuss the nature of the catalysts.

MATERIALS AND METHODS

Preparation of the hammerhead ribozyme and its substrate

The ribozyme (R32) and its substrate (S11) were synthesized chemically on a DNA/RNA synthesizer (model 394; PE Applied Biosystems, Foster City, CA) using phosphoramidic chemistry with 2′-*tert* butyldimethylsilyl (TBDMS) protection as described previously (25). Chemically synthesized oligonucleotides were deprotected in a mixture of 28% ammonia and ethanol (3:1) at 55°C for 8 h. The mixture was evaporated to dryness and the residue was allowed to dissolve in 1 ml of 1 M tetrabutylammonium fluoride (TBAF; Sigma-Aldrich, Japan K.K., Tokyo, Japan) at room temperature for 12 h. After the addition of 1 ml of water, the mixture was desalted on a gel-filtration column (Bio-Gel P-4; Bio-Rad Laboratories, Hercules, CA). Fully deprotected oligonucleotides were purified by gel electrophoresis on a 20% polyacrylamide gel that contained 7 M urea, the respective bands were excised from the gel, and oligonucleotides were extracted in water. The oligonucleotides were recovered by ethanol precipitation and then solutions were desalted on a gel-filtration column (TSK-GEL G3000PW; TOSOH, Tokyo, Japan) by high-performance liquid chromatography (HPLC) with ultrapure water. All of the RNA oligomers were quantitated in terms of absorbance at 260 nm.

The substrate S11 was labeled with [γ-^{32}P]ATP by T4 polynucleotide kinase (Takara Bio, Inc., Shiga, Japan). Radiolabeled S11 was purified on a 20% polyacrylamide gel that contained 7 M urea and then purified by the standard procedure, as described above, with desalting on a gel-filtration column (NAP^{TM}-10 column; Amersham Biosciences, K.K., Tokyo, Japan).

Quantification of the ribozyme reaction

All ribozyme reactions were performed under single-turnover conditions to ensure that conversion of the ribozyme–substrate

complex to the ribozyme–product complex could be monitored kinetically without complications due to complex formation and slow release of products. The solution for the ribozyme reaction contained a trace amount of 5′-^{32}P-labeled S11 and 25 mM Bis-Tris buffer at pH 6.0 and 25°C. The pH values of all 1.25× pre-stock Bis-Tris buffers that contained appropriate metal ions (metal-ion–buffer) were adjusted appropriately with HCl and we confirmed that each buffer had the appropriate pH under the chosen reaction conditions. Each reaction was initiated by addition of the substrate to a mixture of metal-ion–buffer and ribozyme, and aliquots were removed from the reaction mixture at appropriate intervals. Each aliquot was mixed with more than three volumes of a stop solution that contained 100 mM MES (pH 6), 100 mM EDTA, 7 M urea, xylene cyanol (0.1%) and bromophenol blue (0.1%), and then it was stored at −80°C prior to analysis. Since EDTA does not chelate Mg^{2+} and Li^+ ions efficiently at lower pH values, we confirmed that reactions did not continue in the stop solution and that quenching was effective due to high concentration of urea in this solution. Uncleaved substrate and 5′-cleaved products were separated on a 20% polyacrylamide gel that contained 7 M urea. The extent of each cleavage reaction was quantitated with an imageanalyzer (Storm 830; Molecular Dynamics, Sunnyvale, CA). For each reaction, an observed rate constant was determined by non-linear least-squares fitting of the time course of reaction using a pseudo-first-order equation.

RESULTS AND DISCUSSION

The dependence of the activity of the hammerhead ribozyme on the concentration of Li^+ ions

We examined the dependence of the activity of the ribozyme on the concentration of Li^+ ions to confirm that Li^+ ions affect the ribozyme's activity, as reported previously by others (51). We performed reactions under single-turnover conditions at pH 7.5 and 25°C. The results are shown in Figure 2A. Although the activity reached a plateau at ~3 M Li^+ ions, the dependence on the concentration of Li^+ ions was observed (with a slope of three) below the plateau. In the study by O'Rear *et al.* (51), the hammerhead ribozyme reaction exhibited second-order dependence on Li^+ ions up to 4 M at pH 7.5. Although our curve is steeper than the curve that they obtained under the same conditions, with the exception of the concentrations of Li^+ ions, the slopes of both profiles obtained with Li^+ ions are clearly steeper than those of profiles obtained with Mg^{2+} ions. Our profile is unique insofar as we observed saturation of the ribozyme reaction in the range of 3–5 M (Figure 2A). This plateau suggests that the ribozyme reaction might involve the binding of Li^+ ions to the ribozyme–substrate complex.

We also confirmed the dependence on pH, with a slope of unity, of the activity in the presence of a high concentration of Li^+ ions, as shown in Figure 2B. This result supports the hypothesis that the cleavage step is the rate-limiting step even at such a high ionic strength. The pH profile is also consistent with the previous report by Curtis and Bartel (52). As shown in Figure 2A, the observed rate constant at a saturating concentration of Li^+ ions (3–5 M) at pH 7.5 was ~0.17 min^{-1}. The estimated observed rate constant in the

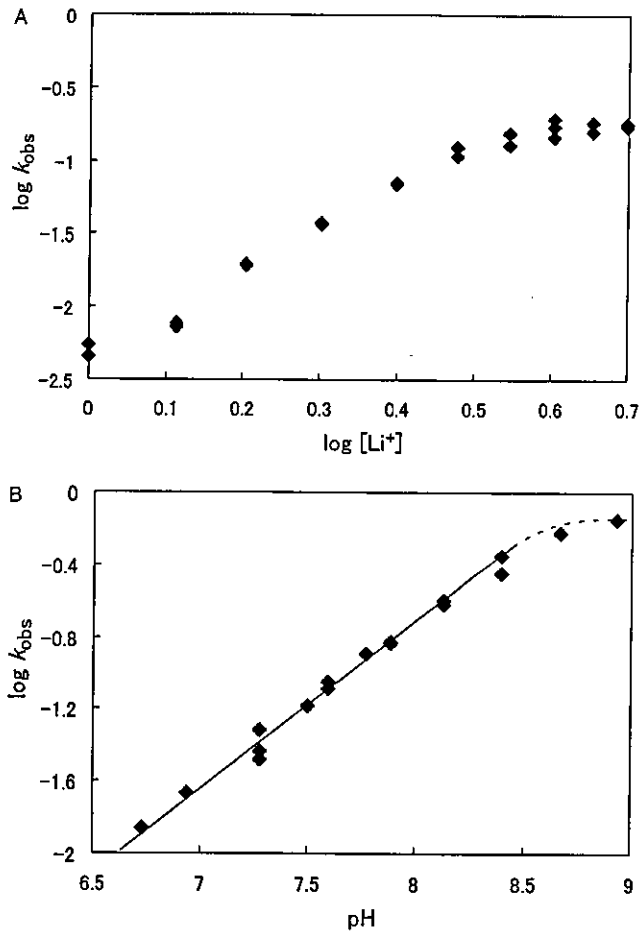

Figure 2. (A) Dependence of cleavage activity on the concentration of Li^+ ions. The activity increased linearly with the concentration of Li^+ ions until ~3 M. Reaction conditions: 25 mM Bis-Tris, pH 7.5, and varying concentrations of Li^+ ions as indicated. (B) Dependence on pH of the activity in 2 M Li^+ ions. The Li^+-containing buffer used in this experiment included Bis-Tris propane and Tris. The cleavage rate increased linearly with pH, yielding a slope of 0.9.

presence of 800 mM Mg^{2+} ions was 32 min^{-1} at pH 7.5, as determined from the value of 1 min^{-1} at pH 6 at the same temperature as that at which the Li^+ experiment was performed (see later). The difference was, thus, approximately 200-fold under similar conditions. The true difference might be even greater because, in contrast to the results with Li^+, the rate at 800 mM Mg^{2+} does not reach a plateau value (see later). These data indicate clearly that Mg^{2+} ions are more suitable for an effective hammerhead ribozyme reaction than any other monovalent ions (Li^+ ions have the highest activity of all monovalent ions in the ribozyme reaction).

The dependence of the activity of the hammerhead ribozyme on the concentration of Mg^{2+} ions

We attempted first to determine how many Mg^{2+} ions might be involved in our model ribozyme reaction and the saturating concentration of Mg^{2+} ions in the reaction, beyond which the cleavage rate constant no longer increases. We examined the dependence on the concentration of Mg^{2+} ions of the activity

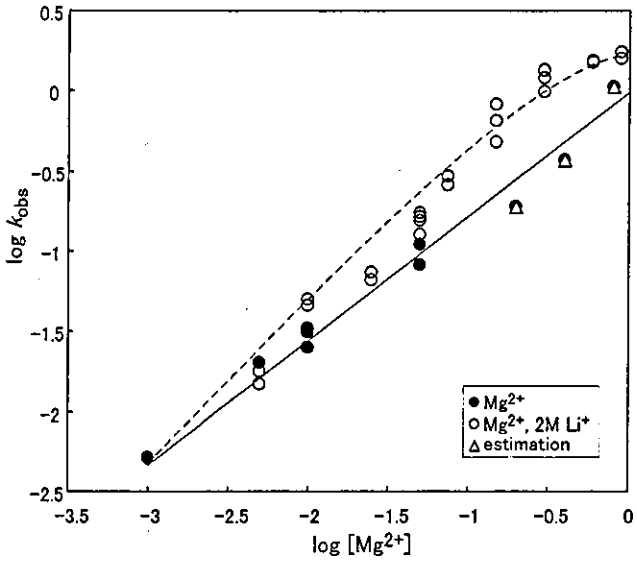

Figure 3. The Mg^{2+}-titration curve for cleavage activity in the presence (open circles) and absence (filled circles) of Li^+ ions. In the absence of Li^+ ions, the line drawn with the linear best fit had a slope of 0.7. The activity increased with increasing concentrations of Mg^{2+} ions and did not reach a plateau value even at 800 mM Mg^{2+} ions. In the presence of 2 M Li^+ ions, the activity increased with increases in the concentration of Mg^{2+} ions up to ~600 mM. Triangles are the calculated rates in the presence of Mg^{2+} ions plus 2 M Li^+ ions, which were determined simply by adding the respective reaction rates together. Since the observed rate in the presence of 2 M Li^+ ions only at pH 6 was <0.01 min^{-1}, triangles are at almost the same positions as the filled circles. The rates observed in the presence of Mg^{2+} ions and Li^+ ions together (open circles) were clearly higher than the calculated values (triangles).

of the R32 hammerhead ribozyme up to ~1 M Mg^{2+} ions. We performed reactions with R32-S11 (Figure 1B) under single-turnover conditions with a saturating amount of ribozyme with respect to the amount of S11 for the same reasons as noted above. The reaction in the presence of Mg^{2+} ions is accelerated with increases in pH, with a slope of unity (7,40,43,44,47,53). We adjusted the pH of reactions to 6.0 to slow down the reaction so that we could determine the rate constants of rapid reactions precisely. As shown by closed circles in Figure 3, the dependence on Mg^{2+} ions was approximately first-order. However, no plateau was reached under our conditions, even above 800 mM Mg^{2+} ions. The continuous increase in rate constant upon the addition of more and more Mg^{2+} ions indicates the involvement of one Mg^{2+} ion that has low affinity for the hammerhead ribozyme–substrate complex. At 800 mM Mg^{2+} ions, the rate constant approached 1.1 min^{-1} at pH 6.0, and this is the limit of detection of a rapid cleavage reaction under standard laboratory conditions.

Analyses of the structure of hammerhead ribozymes and of the conformational changes caused by interactions with Mg^{2+} ions have indicated that two major conformational changes occur: the formation of domain II, which is followed by the formation of domain I, as shown in Figure 1C (38,45, 48,50,54). The formation of domain II results in coaxial stacking of helices II and III, induced by the binding of a higher-affinity Mg^{2+} ion(s) to P9 phosphate and N7 of $G_{10.1}$ (P9/G10.1) of the ribozyme–substrate complex (38,45,48,50,54–58). The second transition is the formation of the catalytic domain with movement of stem I toward stem II, which is induced by the binding of a lower-affinity Mg^{2+} ion(s). The K_d values of the two domains have been determined by various methods to be several hundred micromolar and several millimolar, respectively (45,46,48,50,54). Thus, at several hundred millimolar Mg^{2+} ions, the formation of domains II and I should be complete.

Taking this structural information into consideration, we can reasonably conclude that the very-low-affinity Mg^{2+} ion that we detected in the present study might be involved in some step other than the formation of domains I and II. This step might be a conformational change or the binding of a catalytic species to the ribozyme–substrate complex. Walter and coworkers recently reported that a third and previously undetected metal ion at rather high concentrations might play a role in the induction of a minor conformational adjustment that leads to the formation of the active state after the formation of domains I and II (59). The Mg^{2+} ion that we detected had very low affinity, and the relative level of truly active ribozyme species at a concentration of several millimolar Mg^{2+} ions corresponded to <1% of all the ribozyme–substrate complexes in the reaction mixture [compare 1 min^{-1} in 10 mM $MgCl_2$ at pH 8 and 25°C (60) with 100 min^{-1} in 800 mM $MgCl_2$ at the same pH and the same temperature (see later)].

One might agree that Figure 3 does not support the existence of a very-low-affinity binding site for an Mg^{2+} ion on the ribozyme–substrate complex since the binding curve does not reach a plateau. If the dependence that we observed here were due only to ionic strength, no plateau would be observed. However, we did observe a plateau in the case of Li^+ ions (Figure 2A). Because reactions were so rapid, even at low pH, we could not monitor the kinetics at even higher concentrations of Mg^{2+} ions, such as 3 M. However, it is likely that, in ribozyme reactions, ionic strength is less important than the ion radius and/or the electron density of metal ions since (i) a correlation between the ion radius of Group I monovalent metal ions and ribozyme activity has been observed (52,57) and (ii) an apparent plateau was reached in the presence of high concentrations of Mg^{2+} ions plus 2 M Li^+ ions (Figure 3). Although we cannot calculate a Hill constant for Mg^{2+} ions and estimate the number of binding sites for Mg^{2+} ions from our current data, all the available data strongly support the possibility of the existence of a very-low-affinity metal-binding site(s).

Misra and Draper (61) proposed a model for the stabilization of RNA by Mg^{2+} ions that arises from two distinct binding modes, diffuse binding and site binding. Diffusely bound Mg^{2+} ions are defined as fully solvated ions that interact with RNA only through long-range electrostatic interactions. Site-bound Mg^{2+} ions are defined as partially desolvated ions that are attracted to electronegative pockets. In general, the affinity of diffusely bound Mg^{2+} ions appears to be lower than that of site-bound Mg^{2+} ions. Thus, it is possible that the very-low-affinity Mg^{2+} ions that we detected here might be involved in diffuse binding. Although diffuse binding can sometimes play a dominant role in stabilizing the tertiary structures of small RNAs (61), we cannot exclude the possibility that such diffuse binding Mg^{2+} ion might play a role in catalysis in the ribozyme reaction at a specific site in the ribozyme–substrate complex.

In 800 mM Mg^{2+} ions, the observed rate constant of the reaction catalyzed by the hammerhead ribozyme can be estimated to be ~100 min^{-1} at pH 8 and 25°C, from the

dependence on pH with a slope of unity. The estimated rate constant at concentrations of Mg^{2+} ions >800 mM should be much higher than that at 800 mM since the cleavage reaction did not reach saturation at 800 mM Mg^{2+} and approached the estimated observed rate constant of a 'kissing ribozyme', under saturating conditions with respect to Mg^{2+} ions and pH (62).

The dependence of the activity of the hammerhead ribozyme on Mg^{2+} ions in the presence of a high concentration of Li^+ ions

In order to investigate the properties of Mg^{2+} ions in the ribozyme reaction in further detail, we examined the dependence on Mg^{2+} ions in the presence of a high concentration (2 M) of Li^+ ions. We chose the Li^+ ion as the monovalent cation because this ion is the most active of a large variety of monovalent cations (57). At 2 M Li^+ ions at pH 6.0, the hammerhead ribozyme had detectable activity in the absence of Mg^{2+} ions. We varied the concentration of Mg^{2+} ions from 5 to 900 mM and measured the rate constant. As shown by open circles in Figure 3, we observed approximately first-order dependence on the concentration of Mg^{2+} ions up to 600 mM, and then the rate constant started to reach a plateau from 600 to 900 mM Mg^{2+} ions. These data indicate that, even in the presence of a very high concentration of Li^+ ions, an Mg^{2+} ion with very low affinity plays an important role in the hammerhead ribozyme reaction. The plateau that seemed to appear in the presence of high concentrations of Li^+ ions (Figure 3, open circles) was not observed in the absence of Li^+ ions (closed circles). This apparent plateau was not due to misfolding of RNA at such a high ionic concentration because the extent of cleavage at the end of the reaction was always >90% under these conditions. The plateau might indicate that Li^+ ions help the ribozyme–substrate complex to fold into a more active form, contributing to the enhanced binding of the very-low-affinity Mg^{2+} ion(s) to the complex.

We examined reactions in the presence of Mg^{2+} ions only (Figure 3, closed circles) and in the presence of Li^+ ions only (57). We then calculated rate constants (Figure 3, triangles) on the assumption that Mg^{2+} and Li^+ ions function independently. It should be noted that the observed rate constant in the presence of both Mg^{2+} ions and 2 M Li^+ ions together (Figure 3, open circles) was definitely higher than the calculated rates (Figure 3, triangles) at pH 6 (compare open circles with triangles in Figure 3). One might expect that, in such an experiment (i) the activities in the presence of both metal ions together would be lower than the estimated activities (triangles) because of the lower ability of Mg^{2+} ions to bind to RNA in the presence of high ionic strength due to 2 M Li^+ ions and (ii) the stimulation by Mg^{2+} ions in the presence of such a high concentration of Li^+ ions would be smaller than in the absence of Li^+ ions. It has been reported that stimulation by Cd^{2+} ions is reduced in a ribozyme reaction in the presence of 4 M Li^+ ions (51), while stimulation by Cd^{2+} ions is observed in reaction mixtures that contain 10 mM Ca^{2+} ions instead of 2 M Li^+ ions (23). However, the results in the present study were quite opposite: (i) the activities in the presence of Mg^{2+} ions and 2 M Li^+ ions together (open circles in Figure 3) were higher than the calculated activities (triangles in Figure 3), and (ii) the stimulation by Mg^{2+} ions in the presence of 2 M Li^+ ions (open circles in Figure 3) was even greater than that by Mg^{2+} ions in the absence of Li^+ ions (closed circles in Figure 3).

Our observations suggest the existence of a new cooperative pathway that involves Li^+ and Mg^{2+} ions, in which both metal ions function cooperatively in structural support and/or as the catalyst(s) to increase the rate constant of cleavage (57). In the case of cleavage of RNA by another type of ribozyme, the RNA subunit of RNase P, a similar cooperativity between the metal ions, e.g. Mg^{2+} and Ca^{2+}, has been reported (63).

What is the catalyst in the hammerhead reaction?

To the best of our knowledge, this report is the first to describe the dependence of ribozyme activity on a high concentration of Mg^{2+} ions under single-turnover conditions (Figure 3). The reaction did not reach a plateau even at 800 mM Mg^{2+} ions. Under these conditions at pH 6, the observed rate constant was 1.1 min^{-1}. The activity of the ribozyme is known to depend on pH, with a slope of unity. Thus, we can estimate an observed rate constant for the ribozyme reaction of 110 min^{-1} at pH 8. It is very unlikely that this rate constant of cleavage can occur without an effective catalyst(s) (64). So, what is the catalyst(s) of the reaction?

In studies of solvent isotope effects on the ribozyme reaction in the presence of deuterium and Li^+, Mg^{2+} or NH_4^+ ions, we failed previously to observe any proton transfers in the transition state during the ribozyme reaction in the presence of either Li^+ or Mg^{2+} ions but we did observe proton transfer in the presence of NH_4^+ ions (53,65). We interpreted such results by suggesting that metal ions, such as Mg^{2+} and Li^+, function as a Lewis acid catalyst while NH_4^+ ions function as a general acid catalyst during the ribozyme reaction. Thus, the catalyst can change according to the conditions around the ribozyme. On the basis of this hypothesis and the involvement of two other kinds of Mg^{2+} ions in the formation of domains I and II, it is possible that the newly identified Mg^{2+} ion with very low affinity that we observed in this study might be the true catalyst. Our novel cooperative pathway might involve an Mg^{2+} ion in a catalytic role after monovalent cations and other Mg^{2+} ions have acted to generate the pre-active conformation just before chemical cleavage by the hammerhead ribozyme. In the presence of monovalent ions exclusively, monovalent ions can also function as the catalyst but they are not as effective. Mg^{2+} ions have a higher charge density than Li^+ ions and would function better as catalyst in the reaction. Thus, when both Mg^{2+} and Li^+ ions are present in the reaction mixture, the high activity of the ribozyme reaction is likely due to an Mg^{2+} ion catalyst. The Li^+ ions act to support the formation of the domains I and II in cooperation with Mg^{2+} ions, as discussed above.

We are at present constructing a reaction scheme for ribozyme reactions in the presence of both Mg^{2+} and Li^+ ions, namely, a 'cooperative pathway', by determining the details of the stoichiometric relationships among these metal ions (57). Examination of ribozyme-catalyzed reactions in the presence of various metal ions in combination should clarify the roles of metal ions in catalysis.

ACKNOWLEDGEMENTS

The authors thank Dr Laura Nelson for helpful comments.

REFERENCES

1. Cech,T.R., Zaug,A.J. and Grabowski,P.J. (1981) *In vitro* splicing of the ribosomal RNA precursor of *Tetrahymena*: involvement of a guanosine nucleotide in the excision of the intervening sequence. *Cell*, **27**, 487–496.
2. Guerrier-Takada,C., Gardiner,K., Marsh,T., Pace,N. and Altman,S. (1983) The RNA moiety of ribonuclease P is the catalytic subunit of the enzyme. *Cell*, **35**, 849–857.
3. Symons,R.H. (1992) Small catalytic RNAs. *Annu. Rev. Biochem.*, **61**, 641–671.
4. Carola,C. and Eckstein,F. (1999) Nucleic acid enzymes. *Curr. Opin. Chem. Biol.*, **3**, 274–283.
5. Warashina,M., Zhou,D.M., Kuwabara,T. and Taira,K. (1999) Ribozyme structure and function. In Söll,D., Nishimura,S. and Moore,P.B. (eds), *Comprehensive Natural Products Chemistry*. Elsevier Science Ltd, Oxford, Vol. 6, pp. 235–268.
6. Warashina,M., Takagi,Y., Stec,W.J. and Taira,K. (2000) Differences among mechanisms of ribozyme-catalyzed reactions. *Curr. Opin. Biotechnol.*, **11**, 354–362.
7. Takagi,Y., Warashina,M., Stec,W.J., Yoshinari,K. and Taira,K. (2001) Recent advances in the elucidation of the mechanisms of action of ribozymes. *Nucleic Acids Res.*, **29**, 1815–1834.
8. Noller,H.F., Hoffarth,V. and Zimniak,L. (1992) Unusual resistance of peptidyl transferase to protein extraction procedures. *Science*, **256**, 1416–1419.
9. Nissen,P., Hansen,J., Ban,N., Moore,P.B. and Steitz,T.A. (2000) The structural basis of ribosome activity in peptide bond synthesis. *Science*, **289**, 920–930.
10. Muth,G.W., Ortoleva-Donnelly,L. and Strobel,S.A. (2000) A single adenosine with a neutral pK_a in the ribosomal peptidyl transferase center. *Science*, **289**, 947–950.
11. Cech,T.R. (2000) Structural biology. The ribosome is a ribozyme. *Science*, **289**, 878–879.
12. Collins,C.A. and Guthrie,C. (2000) The question remains: is the spliceosome a ribozyme? *Nature Struct. Biol.*, **10**, 850–854.
13. Hampel,A. and Cowan,J.A. (1997) A unique mechanism for RNA catalysis: the role of metal cofactors in hairpin ribozyme cleavage. *Chem. Biol.*, **4**, 513–517.
14. Nesbitt,S., Hegg,L.A. and Fedor,M.J. (1997) An unusual pH-independent and metal-ion-independent mechanism for hairpin ribozyme catalysis. *Chem. Biol.*, **4**, 619–630.
15. Young,K.J., Gill,F. and Grasby,J.A. (1997) Metal ions play a passive role in the hairpin ribozyme catalysed reaction. *Nucleic Acids Res.*, **25**, 3760–3766.
16. Chowrira,B.M., Berzal-Herranz,A. and Burke,J.M. (1993) Ionic requirements for RNA binding, cleavage, and ligation by the hairpin ribozyme. *Biochemistry*, **32**, 1088–1095.
17. Earnshaw,D.J. and Gait,M.J. (1998) Hairpin ribozyme cleavage catalyzed by aminoglycoside antibiotics and the polyamine spermine in the absence of metal ions. *Nucleic Acids Res.*, **26**, 5551–5561.
18. Seyhan,A.A. and Burke,J.M. (2000) Mg^{2+}-independent hairpin ribozyme catalysis in hydrated RNA films. *RNA*, **6**, 189–198.
19. Uhlenbeck,O.C. (1987) A small catalytic oligoribonucleotide. *Nature*, **328**, 596–600.
20. Haseloff,J. and Gerlach,W.L. (1988) Simple RNA enzymes with new and highly specific endoribonuclease activities. *Nature*, **334**, 585–591.
21. Hutchins,C.J., Rathjen,P.D., Forster,A.C. and Symons,R.H. (1986) Self-cleavage of plus and minus RNA transcripts of avocado sunblotch viroid. *Nucleic Acids Res.*, **14**, 3627–3640.
22. Koizumi,M., Hayase,Y., Iwai,S., Kamiya,H., Inoue,H. and Ohtsuka,E. (1989) Design of RNA enzymes distinguishing a single base mutation in RNA. *Nucleic Acids Res.*, **17**, 7059–7071.
23. Wang,S., Karbstein,K., Peracchi,A., Beigelman,L. and Herschlag,D. (1999) Identification of the hammerhead ribozyme metal ion binding site responsible for rescue of the deleterious effect of a cleavage site phosphorothioate. *Biochemistry*, **38**, 14363–14378.
24. Maderia,M., Hunsicker,L.M. and DeRose,V.J. (2000) Metal–phosphate interactions in the hammerhead ribozyme observed by ^{31}P NMR and phosphorothioate substitutions. *Biochemistry*, **39**, 12113–12120.
25. Yoshinari,K. and Taira,K. (2000) A further investigation and reappraisal of the thio effect in the cleavage reaction catalyzed by a hammerhead ribozyme. *Nucleic Acids Res.*, **28**, 1730–1742.
26. Peracchi,A., Beigelman,L., Scott,E.C., Uhlenbeck,O.C. and Herschlag,D. (1997) Involvement of a specific metal ion in the transition of the hammerhead ribozyme to its catalytic conformation. *J. Biol. Chem.*, **272**, 26822–26826.
27. Knöll,R., Bald,R. and Fürste,J.P. (1997) Complete identification of nonbridging phosphate oxygens involved in hammerhead cleavage. *RNA*, **3**, 132–140.
28. Nakamatsu,Y., Warashina,M., Kuwabara,T., Tanaka,Y., Yoshinari,K. and Taira,K. (2000) Significant activity of a modified ribozyme with N7-deazaguanine at $G_{10.1}$: the double-metal-ion mechanism of catalysis in reactions catalysed by hammerhead ribozymes. *Genes Cells*, **5**, 603–612.
29. Peracchi,A., Beigelman,L., Usman,N. and Herschlag,D. (1996) Rescue of abasic hammerhead ribozymes by exogenous addition of specific bases. *Proc. Natl Acad. Sci. USA*, **93**, 11522–11527.
30. Peracchi,A., Karpeisky,A., Maloney,L., Beigelman,L. and Herschlag,D. (1998) A core folding model for catalysis by the hammerhead ribozyme accounts for its extraordinary sensitivity to abasic mutations. *Biochemistry*, **37**, 14765–14775.
31. Murray,J.B. and Scott,W.G. (2000) Does a single metal ion bridge the A-9 and scissile phosphate groups in the catalytically active hammerhead ribozyme structure? *J. Mol. Biol.*, **296**, 33–41.
32. Tanaka,Y., Morita,E.H., Hayashi,H., Kasai,Y., Tanaka,T. and Taira,K. (2000) Well-conserved tandem G•A pairs and the flanking C•G pair in hammerhead ribozymes are sufficient for capture of structurally and catalytically important metal ions. *J. Am. Chem. Soc.*, **122**, 11303–11310.
33. Suzumura,K., Warashina,M., Yoshinari,K., Tanaka,Y., Kuwabara,T., Orita,M. and Taira,K. (2000) Significant change in the structure of a ribozyme upon introduction of a phosphorothioate linkage at P9: NMR reveals a conformational fluctuation in the core region of a hammerhead ribozyme. *FEBS Lett.*, **473**, 106–112.
34. Tanaka,Y., Kojima,C., Morita,E.H., Kasai,K., Ono,A., Kainosho,M. and Taira,K. (2002) Identification of the metal ion binding site on an RNA motif from hammerhead ribozymes using ^{15}N-NMR spectroscopy. *J. Am. Chem. Soc.*, **124**, 4595–4601.
35. Hansen,M.R., Simorre,J.P., Hanson,P., Mokler,V., Bellon,L., Beigelman,L. and Pardi,A. (1999) Identification and characterization of a novel high affinity metal-binding site in the hammerhead ribozyme. *RNA*, **5**, 1099–1104.
36. Feig,A.L., Panek,M., Horrocks,W.D. and Uhlenbeck,O.C. (1999) Probing the binding of Tb(III) and Eu(III) to the hammerhead ribozyme using luminescence spectroscopy. *Chem. Biol.*, **6**, 801–810.
37. Murray,J.B., Seyhan,A.A., Walter,N.G., Burke,J.M. and Scott,W.G. (1998) The hammerhead, hairpin and VS ribozymes are catalytically proficient in monovalent cations alone. *Chem. Biol.*, **5**, 587–595.
38. Zhou,J.-M., Zhou,D.-M., Takagi,Y., Kasai,Y., Inoue,A., Baba,T. and Taira,K. (2002) Existence of efficient divalent metal ion-catalyzed and inefficient divalent metal ion-independent channels in reactions catalyzed by a hammerhead ribozyme. *Nucleic Acids Res.*, **30**, 2374–2382.
39. Kasai,Y., Shizuku,H., Takagi,Y., Warashina,M. and Taira,K. (2002) Measurements of weak interactions between truncated substrates and a hammerhead ribozyme by competitive kinetic analyses: implications for the design of new and efficient ribozymes with high sequence specificity. *Nucleic Acids Res.*, **30**, 2383–2389.
40. Zhou,D.-M. and Taira,K. (1998) The hydrolysis of RNA: from theoretical calculations to the hammerhead ribozyme-mediated cleavage of RNA. *Chem. Rev.*, **98**, 991–1026.
41. Takagi,Y. and Taira,K. (1995) Temperature-dependent change in the rate-determining step in a reaction catalyzed by a hammerhead ribozyme. *FEBS Lett.*, **361**, 273–276.
42. Koizumi,M. and Ohtsuka,E. (1991) Effects of phosphorothioate and 2-amino groups in hammerhead ribozymes on cleavage rates and Mg^{2+} binding. *Biochemistry*, **30**, 5145–5150.
43. Dahm,S.C., Derrick,W.B. and Uhlenbeck,O.C. (1993) Evidence for the role of solvated metal hydroxide in the hammerhead cleavage mechanism. *Biochemistry*, **32**, 13040–13045.
44. Hendry,P. and McCall,M.J. (1995) A comparison of the *in vitro* activity of DNA-armed and all-RNA hammerhead ribozymes. *Nucleic Acids Res.*, **23**, 3928–3936.
45. Bassi,G.S., Murchie,A.I.H., Walter,F., Clegg,R.M. and Lilley,D.M.J. (1997) Ion-induced folding of the hammerhead ribozyme: a fluorescence resonance energy transfer study. *EMBO J.*, **16**, 7481–7489.
46. Horton,T.E., Clardy,D.R. and DeRose,V.J. (1998) Electron paramagnetic resonance spectroscopic measurement of Mn^{2+} binding affinities to the hammerhead ribozyme and correlation with cleavage activity. *Biochemistry*, **37**, 18094–18101.

47. Peracchi,A. (1999) Origins of the temperature dependence of hammerhead ribozyme catalysis. *Nucleic Acids Res.*, **27**, 2875–2882.
48. Bassi,G.S., Møllegaard,N.E., Murchie,A.I.H. and Lilley,D.M.J. (1999) RNA folding and misfolding of the hammerhead ribozyme. *Biochemistry*, **38**, 3345–3354.
49. Hunsicker,L.M. and DeRose,V.J. (2000) Activities and relative affinities of divalent metals in unmodified and phosphorothioate-substituted hammerhead ribozymes. *J. Inorg. Biochem.*, **80**, 271–281.
50. Hammann,C., Norman,D.G. and Lilley,D.M.J. (2001) Dissection of the ion-induced folding of the hammerhead ribozyme using ^{19}F-NMR. *Proc. Natl Acad. Sci. USA*, **98**, 5503–5508.
51. O'Rear,J.L., Wang,S., Feig,A.L., Beigelman,L., Uhlenbeck,O.C. and Herschlag,D. (2001) Comparison of the hammerhead cleavage reactions stimulated by monovalent and divalent cations. *RNA*, **7**, 537–545.
52. Curtis,E.A. and Bartel,D.P. (2001) The hammerhead cleavage reaction in monovalent cations. *RNA*, **7**, 546–552.
53. Takagi,Y. and Taira,K. (2002) Detection of a proton-transfer process by kinetic solvent isotope effects in NH_4^+-mediated reactions catalyzed by a hammerhead ribozyme. *J. Am. Chem. Soc.*, **124**, 3850–3852.
54. Bassi,G.S., Møllegaard,N.E., Murchie,A.I.H., von Kitzing,E. and Lilley,D.M.J. (1995) Ionic interactions and the global conformations of the hammerhead ribozyme. *Nature Struct. Biol.*, **2**, 45–55.
55. Schiemann,O., Fritscher,J., Kisseleva,N., Sigurdsson,S.T. and Prisner,T.F. (2003) Structural investigation of a high-affinity MnII binding site in the hammerhead ribozyme by EPR spectroscopy and DFT calculations. Effects of neomycin B on metal-ion binding. *ChemBioChem*, **4**, 1057–1065.
56. Tanaka,Y., Kasai,Y., Mochizuki,S., Wakisaka,A., Morita,E.H., Kojima,C., Toyozawa,A., Kondo,Y., Taki,M., Takagi,Y., Inoue,A., Yamasaki,K. and Taira,K. (2004). Nature of the chemical bond formed with the structural metal ion at the A9/G10.1 motif derived from hammerhead ribozymes. *J. Am. Chem. Soc.*, **126**, 744–752.
57. Takagi,Y., Inoue,A. and Taira,K. (2004). Analysis of on a cooperative pathway involving multiple cations in hammerhead reactions. *J. Am. Chem. Soc.*, in press.
58. Warashina,M., Kuwabara,T., Nakamatsu,Y., Takagi,Y., Kato,Y. and Taira,K. (2004) Analysis of the conserved P9-G10.1 metal binding motif in hammerhead ribozymes with extra nucleotide inserted between A9 and G10.1 residues. *J. Am. Chem. Soc.*, in press.
59. Rueda,D., Wick,K., McDowell,S.E. and Walter,N.G. (2003) Diffusely bound Mg^{2+} ions slightly reorient stems I and II of the hammerhead ribozyme to increase the probability of formation of the catalytic core. *Biochemistry*, **42**, 9924–9936.
60. Stage-Zimmermann,T.K. and Uhlenbeck,O.C. (1998) Hammerhead ribozyme kinetics. *RNA*, **4**, 875–889.
61. Misra,V.K. and Draper,D.E. (2002) The linkage between magnesium binding and RNA folding. *J. Mol. Biol.*, **317**, 507–521.
62. Khvorova,A., Lescoute,A., Westhof,E. and Jayasena,S.D. (2003) Sequence elements outside the hammerhead ribozyme catalytic core enable intracellular activity. *Nature Struct. Biol.*, **10**, 708–712.
63. Brännvall,M. and Kirsebom,L.A. (2001) Metal ion cooperativity in ribozyme cleavage of RNA. *Proc. Natl Acad. Sci. USA*, **98**, 12943–12947.
64. Li,Y. and Breaker,R.R. (1999) Kinetics of RNA degradation by specific base catalysis of transesterification involving the 2′-hydroxyl group. *J. Am. Chem. Soc.*, **121**, 5364–5372.
65. Sawata,S., Komiyama,M. and Taira,K. (1995) Kinetic evidence based on solvent isotope effects for the nonexistence of a proton-transfer process in reactions catalyzed by a hammerhead ribozyme—implication to the double-metal-ion mechanism of catalysis. *J. Am. Chem. Soc.*, **117**, 2357–2358.

Accelerated Publication

THE JOURNAL OF BIOLOGICAL CHEMISTRY
Vol. 279, No. 37, Issue of September 10, pp. 38083–38086, 2004

Identification of Metastasis-related Genes in a Mouse Model Using a Library of Randomized Ribozymes*

Received for publication, July 1, 2004
Published, JBC Papers in Press, July 9, 2004,
DOI 10.1074/jbc.C400313200

Eigo Suyama‡§¶, Renu Wadhwa§¶, Kamaljit Kaur§, Makoto Miyagishi‡§, Sunil C. Kaul§, Hiroaki Kawasaki‡§, and Kazunari Taira‡§‖

From the ‡Department of Chemistry and Biotechnology, School of Engineering, The University of Tokyo, 7-3-1 Hongo, Bunkyo-ku, Tokyo 113-8656, Japan and the §Gene Function Research Center, National Institute of Advanced Industrial Science and Technology (AIST), Central 4, 1-1-1 Higashi, Tsukuba Science City, Ibaraki 305-8562, Japan

Libraries of randomized ribozymes have considerable potential as tools for the identification of functional genes critically involved in a biological phenotype of interest *in vitro*. We have used a ribozyme library in an *in vivo* mouse model to identify genes related to metastasis. We injected weakly metastatic melanoma cells that had been treated with the library intravenously into mice. We then isolated ribozymes that accelerated metastasis from pulmonary tumors that had developed from metastasizing cells. As candidates for metastasis-related genes that were targets of the isolated ribozymes, we identified five unknown and three known genes: stromal interaction molecule 1 (*STIM1*), polymerase γ2 accessory subunit (*Polg2*), and cytochrome P450, family 2, subfamily d, polypeptide 22 (*Cyp2d22*). Repression of four of these by small interfering RNAs indeed resulted in the accelerated mobility of cells in *in vitro* scratch-wound assay. The further characterization of these candidate genes would provide clues to the complex mechanism(s) of metastasis.

Hammerhead ribozymes (referred to herein after as ribozymes) that specifically cleave the transcripts of particular genes can be produced when the nucleotide sequences of the substrate-recognition arms are designed such that they are complementary to the sequences of individual target mRNAs. Such ribozymes have been used successfully to interfere with the expression of specific genes via cleavage of the respective target mRNAs in mammalian cells (1–6). The use of a library of ribozymes with randomized substrate-recognition arms allowed the identification of genes that are involved directly in certain phenomena, such as the transformation of NIH3T3 fibroblasts, anchorage-independent cell growth, tumor necrosis factor-α-induced apoptosis and tumor invasion (7–15).

The metastatic spread of tumor cells around the body is a key target for cancer therapy (16, 17). An experimental assay of metastasis *in vivo* that involves intravenous injection of tumor cells into mice was developed by Fidler (18) for the analysis of the metastatic properties of melanoma cells (Fig. 1). In this assay, cells of interest are injected into the tail vein of mice and allowed to proliferate and/or metastasize. After several weeks, pulmonary metastases are observed in the case of strongly metastatic melanoma cells, while relatively few metastases are formed after injection of cells with limited metastatic potential. This assay allows the selection of strongly metastatic cells from a heterogeneous population of weakly metastatic tumor cells (18, 19). Thus, the assay allows not only the study of the metastatic characteristics of melanoma cells but also the isolation of strongly metastatic cells. In the present study, we used this mouse model and mouse B16F0 melanoma cells, a weakly metastatic melanoma cell line, to investigate the applicability of a library of ribozymes *in vivo*, to isolate ribozymes that converted weakly metastatic melanoma cells to strongly metastatic cells by the apparent disruption of expression of specific gene(s), and to identify genes related to metastasis.

EXPERIMENTAL PROCEDURES

Construction of a Ribozyme Library—A library of ribozymes was constructed based on the retrovirus expression vector pMXpuro (20). First, fragments of DNA carrying randomized hammerhead ribozymes were obtained by PCR amplification using oligonucleotide DNAs as follows, a sense primer (5′-TCC CCG GTT CGA AAC CGG GCA-3′), an antisense primer (5′-GCT TGC ATG CCT GCA GGT CGA CGC GAT AGA AAA AAA GAT ATC CGG GGT-3′), and a template (5′-TCC CCG GTT CGA AAC CGG GCA CTA CAA AAA CCA ACT TTN NNN NNNN CTG ATG AGG CCG AAA GGC CGA AAN NNN NNNG GTA CCC CGG ATA TCT TTT TTT-3′, where N represents A, T, G, or C). The fragments were cloned into a plasmid vector, pGEM-T (Promega, Madison, WI), then were digested with Csp45I and KpnI, and were again cloned into pPUR-KE (21). Next, fragments encoding $tRNA^{Val}$-fused randomized ribozymes were obtained by digestion of the library of ribozymes based on pPUR-KE with EcoRI and BamHI. Finally, the fragments were inserted into the EcoRI and BamHI sites in pMXpuro.

Cell Culture and Retroviral Infection—B16F0 melanoma cells (number CRL-6322; ATCC, Manassas, VA) were cultured in Dulbecco's modified Eagle's medium (Sigma) supplemented with 10% fetal bovine serum (Invitrogen) and an antibiotics mixture (Invitrogen). Retroviral preparation and infection with the retroviral vector pMXpuro and the packaging cell line Plat-E (kindly provided by Professor Toshio Kitamura, Institute of Medical Science, University of Tokyo, Tokyo, Japan) were performed as described elsewhere (14, 20). Infected cells were treated with medium that contained puromycin (1 μg/ml, Sigma) for 4 weeks.

Experimental Metastasis Assay—5×10^5 of B16F0 cells, infected with retroviruses carrying a ribozyme library or not, were suspended in phosphate-buffered saline (PBS[1]; Takara Bio, Shiga, Japan) and intravenously injected into the lateral tail vein of C57BL/6NCrj mice (Charles River Japan, Yokohama, Japan). Two weeks after injection, lungs were removed from the mice and were washed with ice-cold PBS. The pulmonary metastases on the surface of the lungs were observed and counted. Then the nodules were removed, minced, and cultured in dishes.

RT-PCR Analysis and Ribozyme Rescue—Total RNA was prepared from cells using the Isogen reagent (Nippon Gene, Toyama, Japan) according to the manufacturer's protocol. cDNA was synthesized using

* The costs of publication of this article were defrayed in part by the payment of page charges. This article must therefore be hereby marked "*advertisement*" in accordance with 18 U.S.C. Section 1734 solely to indicate this fact.

¶ These authors contributed equally to this work.

‖ To whom correspondence should be addressed: Dept. of Chemistry and Biotechnology, School of Engineering, The University of Tokyo, 7-3-1 Hongo, Bunkyo-ku, Tokyo 113-8656, Japan. Tel.: 81-3-5841-8828; Fax: 81-3-5841-8828; E-mail: taira@chembio.t.u-tokyo.ac.jp.

[1] The abbreviations used are: PBS, phosphate-buffered saline; RT, reverse transcriptase; siRNA, small interfering RNA; *STIM1*, stromal interaction molecule 1 gene; *Polg2*, polymerase γ2 accessory subunit gene; *Cyp2d22*, cytochrome P450, family 2, subfamily d, polypeptide 22 gene.